NASA TECHNICAL MEMORANDUM

NASA TM X-64998

SKETCH OF A UNIFYING AURORAL THEORY

By Walter Lennartsson
Space Sciences Laboratory

November 1975

NASA

George C. Marshall Space Flight Center
Marshall Space Flight Center, Alabama

TECHNICAL REPORT STANDARD TITLE PAGE

1. REPORT NO.	2. GOVERNMENT ACCESSION NO.	3. RECIPIENT'S CATALOG NO.
NASA TM X-64998		

4 TITLE AND SUBTITLE	5. REPORT DATE
Sketch of a Unifying Auroral Theory	November 1975
	6. PERFORMING ORGANIZATION CODE

7. AUTHOR(S)	8. PERFORMING ORGANIZATION REPORT #
Walter Lennartsson*	

9. PERFORMING ORGANIZATION NAME AND ADDRESS	10. WORK UNIT NO.
George C. Marshall Space Flight Center Marshall Space Flight Center, Alabama 35812	11. CONTRACT OR GRANT NO.
	13. TYPE OF REPORT & PERIOD COVERED
12 SPONSORING AGENCY NAME AND ADDRESS National Aeronautics and Space Administration Washington, D.C. 20546	Technical Memorandum
	14. SPONSORING AGENCY CODE

15. SUPPLEMENTARY NOTES
Prepared by Space Sciences Laboratory, Science and Engineering
*NAS/NRC Postdoctoral Research Associate, Permanent Address: The Royal Institute of Technology, Dept. of Plasma Physics, S-10044 Stockholm 70, Sweden

16. ABSTRACT

On the basis of field and particle observations, it is suggested that a bright auroral display is a part of a magnetosphere-ionosphere current system which is fed by a charge-separation process in the outer magnetosphere (or the solar wind). The upward magnetic-field-aligned current is flowing out of the display, carried mainly by down-flowing electrons from the hot-particle populations in the outer magnetosphere (the ambient cold electrons being depleted at high altitudes). As a result of the magnetic mirroring of these downflowing current carriers, a large potential drop is set up along the magnetic field, increasing both the number flux and the kinetic energy of the precipitating electrons. It is found that this simple basic model, when combined with wave-particle interactions, may be able to explain a highly diversified selection of auroral particle observations. It may thus be possible to explain both "inverted-V" events and auroral rays in terms of a static parallel electric field, and the electric field may be compatible with a strongly variable pitch-angle distribution of the precipitating electrons, including distributions peaked at 90° as well as 0°. This model may also provide a simple explanation of the simultaneous precipitation of electrons and collimated positive ions.

17. KEY WORDS	18. DISTRIBUTION STATEMENT
	Unclassified — Unlimited Walter Lennartsson

19. SECURITY CLASSIF. (of this report)	20. SECURITY CLASSIF. (of this page)	21. NO. OF PAGES	22. PRICE
Unclassified	Unclassified	57	NTIS

ACKNOWLEDGMENTS

The author acknowledges many fruitful discussions with Drs. J. L. Burch, C. R. Chappell, S. E. DeForest, D. L. Reasoner, and G. R. Swenson of the Marshall Space Flight Center, Huntsville, as well as Dr. L. P. Block and Prof. C. G. Fälthammar of the Royal Institute of Technology, Stockholm.

This work was carried out while the author was an NAS/NRC Resident Research Associate at the George C. Marshall Space Flight Center. The support from NRC and MSFC is gratefully acknowledged.

TABLE OF CONTENTS

LIST OF ILLUSTRATIONS

NOMENCLATURE

α	angle between a particle's velocity vector and the magnetic field (pitch angle)
B	magnetic field strength
$\bar{B}$	magnetic field vector
ΔV	electric potential difference
$(\Delta V)_{\parallel}$	electric potential difference along $\bar{B}$
E	electric field strength
$\bar{E}$	electric field vector
$E_{\parallel}$	electric field component parallel to $\bar{B}$
$E_{\perp}$	electric field component transverse to $\bar{B}$
E_0	a given constant electric field
$\tilde{E}_z$	the vertical electric field averaged over h (vertical distance)
e	the charge of an electron
$\text{grad}_{\parallel} B$	gradient of B along $\bar{B}$
h	vertical distance between two certain altitudes
i	electric current density
$\bar{i}$	electric current density vector
$i_{\parallel}$	electric current density along $\bar{B}$
$i_{\perp}$	electric current density transverse to $\bar{B}$

NOMENCLATURE (Continued)

I	sheet-current density (A/m)
κ	constant
m	particle mass
m_e	the mass of an electron
m_p	the mass of a proton
μ	magnetic moment $mv_\perp^2/2B$
n	electron density
R	radial distance from the center of the Earth
R_e	the radius of the Earth
$\tilde{\sigma}_\parallel^{-1}$	the resistivity parallel to $\bar{B}$ averaged over h
σ	electric conductivity
$\sigma_\parallel$	electric conductivity parallel to $\bar{B}$
$\sigma_\perp$	electric conductivity transverse to $\bar{B}$
σ_P	Pedersen conductivity
σ_H	Hall conductivity
Σ_P	height-integrated Pedersen conductivity
Σ_H	height-integrated Hall conductivity
θ	magnetic co-latitude

NOMENCLATURE (Concluded)

v	velocity
$v_{\parallel}$	velocity parallel to $\bar{B}$
$v_{\perp}$	velocity transverse to $\bar{B}$
v_n	neutral gas velocity
V	electric potential

TECHNICAL MEMORANDUM X-64998

SKETCH OF A UNIFYING AURORAL THEORY

I. INTRODUCTION

One of the most puzzling problems in magnetospheric physics today is how to understand the complex processes that cause energization and precipitation of the auroral particles. A great variety of ideas have been presented in the literature to explain different observed phenomena, but very little has been achieved in obtaining a unified picture. Reference 1 presents an illustration of the complexity of auroral particle observations.

The purpose of this report is to show that the theory of magnetic mirroring may form the basis of an auroral theory that is unifying in the sense that it may explain even seemingly contradictory observations. The reader who only wants a brief orientation may read Sections II, XIV, and XV.

For reference purposes a rough division of current ideas concerning auroral particle acceleration is needed. The main ideas may be grouped into the following three basic categories:

(a.) The precipitating particles have already attained their final energy when leaving the equatorial region of the magnetosphere. It is frequently assumed that the auroral particles get their final energy by, for instance, betatron and Fermi acceleration during their drift motion into and filling the plasma sheet reservoir of energetic particles. For a sufficient flux of the energized particles to reach down to the atmosphere, despite the strong mirroring effect of the geomagnetic field, a final pitch-angle scattering mechanism (by means of wave-particle interactions) may be needed [2]. Some measurements of the near-Earth plasma sheet seem to indicate a sufficient energy flux of particles with appropriate energies for producing even the most intense auroral precipitation [3,4]. Reference 5 presents a very brief review of this kind of large scale energization.

(b.) The precipitating particles in general, or at least some of them, gain additional energy at the expense of a trapped particle component through which they pass on the way down. Alternatively, this energy transfer may be

from one precipitating component to the other. According to this view, the energy-yielding particles having an unstable velocity distribution produce plasma waves, the energy of which is absorbed by the precipitating particles in an ordered manner. A crucial point is then to have the precipitating particles increase preferentially their downward field-aligned velocity [6-9].

(c.) The precipitating particles fall through an electrostatic potential gradient along the magnetic field lines. This requires a drastic reduction of the parallel current-carrying capability of the magnetospheric-ionospheric plasmas relative to what has been normally assumed. The behavior of laboratory plasmas has caused people to think in terms of potential double layers [10,11] or wave-particle generated anomalous resistivity [12,13] as the means by which field-aligned currents are obstructed in auroral regions. Alternatively, the magnetic mirroring may play a key role as demonstrated by Knight [14] and Lemaire and Scherer [15, 16].

II. ESSENTIAL FEATURES OF A NEW MODEL

The model outlined in this report basically belongs to category (c), but important features of it are taken from categories (a) and (b). The basic line of thought is the following.

From curl $\bar{E} = 0$, it is seen that an electrostatic potential gradient along the geomagnetic field lines will be associated with an increased peak amplitude of $E_\perp$ at high altitudes. For the high-altitude $E_\perp$ to stay at reasonable values, the region with a parallel potential drop of several kV must have a fairly wide spatial extent transverse to the magnetic field, in accordance with the observed latitudinal thickness of "inverted-V" events, which is typically 100 to 300 km. This means that thin auroral precipitation structures such as auroral rays must be the result of a local reduction of the parallel "resistivity" rather than a current-induced local increase of the resistivity. This problem may be solved in terms of the following model. The upward field-aligned portion of a magnetosphere-ionosphere current system will be associated with a depletion of ambient cold electrons at high altitudes and, hence, the upward current will be carried by downflowing hot and dilute magnetospheric electrons. Because the parallel motion of these electrons is strongly hampered by the magnetic mirroring, a large fraction of the total voltage produced by the magnetospheric "dynamo" will be projected along the magnetic field, increasing the flux density and the kinetic energy of the downflowing hot electrons. This field-aligned

potential drop may be concentrated mainly to the region of strong magnetic field within approximately one earth radius above the ionosphere. The effective "resistivity" may then be locally reduced by gyroresonant wave-particle interactions reducing the magnetic moment of the electrons. In this manner very thin substructures of increased precipitation may occur, energized by the parallel electric field; that is, in reality by the magnetospheric dynamo.

This report emphasizes the merits of the previously discussed model in explaining a large variety of observed phenomena, but it does not discuss the detailed physical conditions for the wave-particle interactions.

III. SOME OBSERVATIONAL INDICATIONS OF A LARGE $(\Delta V)_{||}$

The observation traditionally considered as indicative of field-aligned potential gradients is that of a "nearly monoenergetic" peak in the energy spectrum of precipitating electrons [1,17-20].

The frequently observed collimation (along $\bar{B}$) of auroral electron distributions is often interpreted in terms of a field-aligned acceleration at low altitudes which may be due to a $(\Delta V)_{||}$ [1, 20-24]. Detailed measurements of pitch-angle versus energy have also led to an interpretation in terms of field-aligned potential gradients [20] or, even more specifically, in terms of double layers [18].

The large amount of satellite data on inverted-V precipitation structures [25] and associated irregularities in the convection electric field [26] observed in the poleward part of the auroral ovals also seem to point in the direction of potential gradients along the magnetic field. These observations will be more extensively discussed in Section XIV.

Direct evidence for a large $(\Delta V)_{||}$ above an auroral form has been found recently from the drift motion of a barium plasma jet injected along the magnetic field lines [27]. While the barium plasma beyond 1 R_e experienced flux tube splitting and rapid dispersion, the plasma at lower altitudes remained unaffected, thus indicating a large variation with altitude of $E_{\perp}$ associated with a large $(\Delta V)_{||}$.

IV. MAGNETIC-FIELD-ALIGNED CURRENTS

Among the different theories of auroral particle acceleration, those involving parallel electric fields seem to be particularly encouraged by the existence of magnetic field-aligned currents. This can be seen by the following arguments.

According to the viewpoints (a) and (b) listed in the Introduction, the auroras are, in fact, produced by a magnetospheric electron gun. The negative charge carried by the electron beam need not give rise to a net field-aligned current, however, because the negative charge thus deposited deep within the ionosphere will enable ionospheric electrons in the topside region to escape outward along the beam (together with backscattered and secondary electrons). Actually, this is what should be expected according to the kinetic model discussed by Lemaire and Scherer [15, 16]. In this way a net field-aligned current may not appear until the precipitation flux density exceeds the flux density of freely escaping ionospheric electrons, which is quite high — maybe as high as 10^{11} $cm^{-2}s^{-1}$ (or more) at ionospheric altitudes [15,16]. In the absence of precipitated negative charges, the outflowing ionospheric electrons are tied to the much slower positive ionospheric ions (ambipolar diffusion).

The situation is quite different when viewpoint (c) is considered. We note that a potential gradient along magnetic field lines in a direction to accelerate precipitating electrons is an efficient barrier to the upward escaping thermal electrons from the ionosphere (actually a potential barrier of only a few volts will do) [15,16] as well as a barrier to backscattered and secondary electrons. Consequently, if the flux of precipitating protons is negligible as compared with the electron flux (as is normally the case [25]), the net $i_{\parallel}$ has to be in the upward direction and at least as large as the current density carried by the precipitating electrons (not including the downflowing electrons that have been reflected by the potential barrier). Likewise, if the net $i_{\parallel}$ is found to be at least as large as the precipitation current density, the most immediate interpretation is that the ionosphere, at the point of deposit of negative charge, stays at a positive potential relative to the adjacent magnetosphere. This potential distribution is easy to understand if the precipitating electrons are passive carriers of current. However, as discussed in Section VIII, the energetic precipitating electrons do not readily act as passive current carriers unless they are forced to by an $e(\Delta V)_{\parallel}$ which is at least of the same order of magnitude as the kinetic energy of the electrons. The reason for this reluctance is the magnetic mirroring in the geomagnetic field. A $(\Delta V)_{\parallel}$ of this magnitude will evidently appreciably increase the energy of the electrons at the same time.

The permanent existence of east-west extended field-aligned current sheets in all local time sectors of the auroral ovals is fairly well established [28,29,30]. It is interesting that an upward $i_{||}$ (downgoing electrons) measured by means of its distortion of the geomagnetic field is very often seen directly associated with precipitating electrons and auroral arcs and that the current density is seemingly at least as high as defined by the precipitation flux density [19,20,31-34].

V. SOME CRUCIAL PROPERTIES OF $(\Delta V)_{||}$

In the theories presented so far concerning potential double layers [10, 11,35], anomalous (turbulent) resistivity [13,36] and the effect of a magnetic mirror [14,37-39], the analysis is restricted to a one-dimensional geometry. When these are applied to the auroral problem, we might expect some complexities to arise as a result of the two- and three-dimensional inhomogeneities in auroral displays (Fig. 1). The left part of the figure, a, is a rough sketch of the well-known electric field generated at a resistant section of an otherwise good conductor when a current is flowing, in this case in the upward direction. The region outside of the conductor is supposed to be a vacuum. The conductor in Figure 1a may be an unmagnetized plasma column contained within a glass tube, and the "resistant" section may be a potential double layer (see the laboratory experiments summarized by Block [40]). The plasma confinement may as well be due to an external axial magnetic field, of course.

Consider now b part of Figure 1 which is a sketch of the formal auroral analogy of Figure 1a. For simplicity the total magnetic field (geomagnetic field and superposed field due to the current) is assumed to be vertical and homogeneous, $B \equiv B_z$. A current is assumed flowing upwards, carried by downward moving electrons and having a density i_z. This current is partly obstructed by a region of reduced parallel "conductivity" $\sigma_{||}$. The word "conductivity" here simply means the quantity i_z/E_z.

In the auroral case there is obviously no vacuum outside of the current path. Hence, the fan-shaped equipotentials in Figure 1a transform into magnetic-field-aligned equipotentials as indicated in Figure 1b. That is, one medium is considered where $E_z = 0$, except for one subregion where $E_z \neq 0$. Now suppose

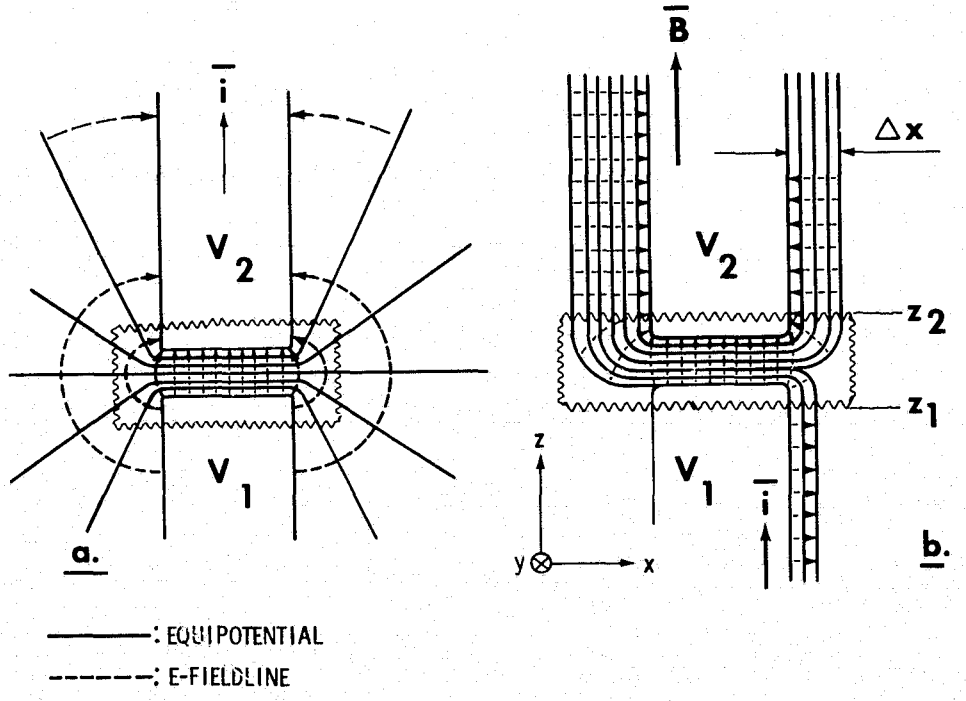

a. The schematic electric field lines and equipotentials created at a resistant portion of an otherwise good conductor when a current is flowing (the surrounding medium is vacuum).

b. The formal analogue when the resistor is a subregion of low conductivity within a magnetized plasma.

Figure 1. Two- and three-dimensional inhomogeneities in auroral displays.

that the wavy contour in Figure 1b indicates the smallest possible box containing the region $E_z \neq 0$. Evidently, E_x is not confined to the immediate vicinity of the box as in Figure 1a but penetrates infinitely far out along $\bar{B}$.

Let us further suppose that the electric field is approximately static:

$$\text{curl } \bar{E} \approx 0 \quad . \tag{1}$$

If we integrate partly the y-component of equation (1) with respect to z, then

$$E_x(x, z_2) - E_x(x, z_1) = \frac{\partial}{\partial x} [V(x, z_1) - V(x, z_2)] \ . \qquad (2a)$$

With reference to Figure 1b this can be written as

$$\left| E_x(z_2) - E_x(z_1) \right|_{max} = \left| \frac{V(z_1) - V(z_2)}{\Delta x} \right|_{max} \ . \qquad (2b)$$

Hence, if the extreme values of $E_\perp$ are known, then the highest possible values of $(\Delta V)_\parallel / \Delta x$ are known. That is, the larger $(\Delta V)_\parallel$ is, the larger is Δx.

This result can easily be generalized to a case with a dipolar total magnetic field where $E_\parallel$ is widely distributed along a magnetic field line. If the longitudinal component of (1) is integrated along a magnetic field line from the equatorial plane down to the ionosphere, utilizing orthogonal dipolar coordinates [41], then we obtain

$$\left(\frac{\partial}{\partial s_\perp} \Delta V_\parallel \right)_{ia} = E_{\perp\, ia} - \frac{R_{ep}^2}{R_{ia}^2} \cdot f(\theta) \cdot E_{\perp\, ep} \qquad (2c)$$

where, the symbol $E_\perp$ is used for the southward component of the transverse electric field; the index "ia" denotes an ionospheric altitude and "ep" the equatorial plane; R is the respective radial distance from the center of the earth; $\Delta V_\parallel = V_{ep} - V_{ia}$ and $s_\perp$ is the southward horizontal ($\perp \bar{B}$) length-coordinate at the ionospheric altitude; θ is the magnetic co-latitude of the ionospheric intersection of the field line; and

$$f(\theta) = (1 + \frac{1}{4} \tan^2\theta)^{1/2} \cdot (2 \sin\theta \cos\theta + \frac{1}{2} \tan\theta \sin^2\theta)^{-1}$$

that is, $f(\theta) \approx 0.7$ with $\theta \approx 20°$.

From equation (2b) it is readily concluded that the common ray structure in visible auroras cannot be directly related to the spatial (transverse to $\bar{B}$) distribution of $(\Delta V_{\parallel})$. In fact, the ray structure might indicate a $\Delta x \lesssim 10^2$ m [42]. A typical energy of the precipitating ray electrons may be 5 keV; that is, $(\Delta V)_{\parallel} \sim 5$ kV would be expected. As seen from equation (2b), this would then require $E_x = E_{\perp} \gtrsim 50$ V/m, which is seemingly impossible [26]. If equation (2c) is considered, peak values of $E_{\perp} \sim 700$ mV/m at $R \sim 10$ earth radii are required. This is highly unrealistic, too, even though very little is known about $E_{\perp}$ in the outermost magnetosphere. The ray structure is further discussed in Section IX.

Equations (2a) through (2c) place a severe restriction on any mechanism that may generate "anomalous resistivity" as a result of high field-aligned current densities. This is particularly true of any mechanism that operates at relatively low altitudes, because it is known from satellite observations that $E_{\perp}$ is, at most, approximately 150 mV/m in the low magnetosphere [26]; therefore, the following conclusion is made: an observed total horizontal thickness of a field-aligned current sheet of less than 10 km automatically excludes any low altitude (only a few thousand km) acceleration of electrons to keV energies by means of a current-generated $E_{\parallel}$. This can be seen to hold true also in the case of a nonvanishing curl $\bar{E}$.

When trying to apply a particular model of current-driven plasma instability to the auroral problem, we may face an unattainable compromise because the instability may require a high value of i_z, while equations (2a) through (2c) require the field-aligned current to be spread out, and the capability of the ionosphere to carry horizontal currents is limited:

$$\bar{i}_{\perp} = \sigma_P (\bar{E}_{\perp} + \bar{v}_n \times \bar{B}) + \sigma_H \cdot \bar{B} \times (\bar{E}_{\perp} + \bar{v}_n \times \bar{B})/B \qquad (3)$$

where $\bar{v}_n$ denotes the neutral gas velocity [43].

If equation (3) is integrated with respect to altitude, we get the total current per meter that can be fed into the ionosphere by means of a field-aligned, sheet-current density $I_{\parallel}$. Roughly speaking, we may

equate for instance $\Sigma_p \cdot E_\perp$ to $2\Delta x \cdot i_\parallel$, where Σ_P is the height integrated σ_P. The largest possible value of Σ_P is probably approximately 40 S [43], and this together with $E_\perp = 150$ mV/m then gives an absolute upper limit of $I_\parallel \sim 6$ A/m. However, this is probably far too much, because $E_\perp$ tends to be reduced where Σ_p (and Σ_H) is large [44-46]. A more realistic maximum value of $I_\parallel$ is rather an order of magnitude lower, in accordance with the magnetic measurements made by Zmuda et al. [28]. These authors infer the values 0.02 to 0.7 A/m for $I_\parallel$. The highest reported values of $i_\parallel$ are approximately $2 \cdot 10^{-4}$ A/m^2 [22]. Using this value for $i_\parallel$ and 0.7 A/m for $I_\parallel$, we get $2\Delta x \sim 3$ km; therefore, we conclude that any instability that does require $i_\parallel$ of at least 10^{-4} A/m^2 to be operating in the ionosphere or lower magnetosphere is highly unlikely to be the actual cause of a $(\Delta V)_\parallel$ of several kV.

It may be different if $E_\parallel$ is distributed all along a magnetic field line, because of the scaling factor in equation (2c). It is seen that $E_\perp$ has to be only a few mV/m at a distance of some ten earth radii for a 10 km thick current sheet of keV electrons at ionospheric altitudes to be fully compatible, in the above sense, with a total $\Delta V_\parallel$ in the kV-range. However, a completely different approach is tried in Section VIII.

VI. A SIMPLE ILLUSTRATION

The simple model presented here will serve as a further illustration of the previous section. As our a priori information about $E_\perp$, a simplified horizontal distribution that is basically similar to the $E_\perp$ distribution seen at auroral latitudes by a polar orbiting satellite at approximately 500 to 2500 km altitude is assumed [26].

According to the observations, the convection directions are generally magnetically eastward or westward, except for stagnation lines near noon and midnight, with essentially antisunward components over the polar cap down to approximately 70° to 80° magnetic latitudes, where a flow reversal is found, and sunward components between this "electric field reversal" and the plasmapause. The reversal is frequently very distinct, although there may sometimes be a gradual transition zone and sometimes a very irregular zone with multiple reversals.

Figure 2 refers to the local evening side of the northern auroral zone. The z-axis points vertically upward, the x- and y-axes point geomagnetically northward and westward, respectively. Again, the total magnetic field $\bar{B}$ is assumed to have straight and vertical field lines. Actually, the current-induced magnetic field is, at most, a few percent of the total field in the low magnetosphere [29].

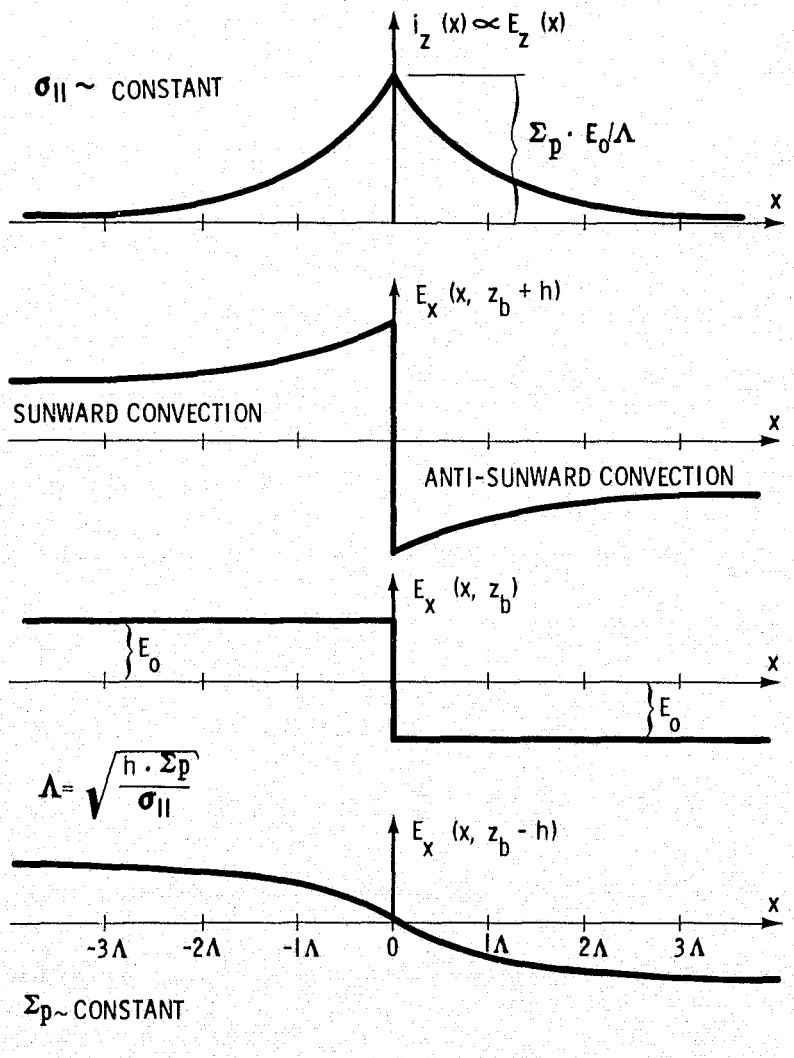

Figure 2. The electric field and current distributions at different altitudes associated with a given distribution of $E_{\perp} = E_x$ at altitude z_b, where z_b is assumed to be in the topside ionosphere or low magnetosphere [the magnetic field is vertical and downward (antiparallel to the z-axis)].

Let us suppose that we know the convection at altitude z_b in the upper ionosphere to be magnetically eastward and westward, that is, parallel to the y-axis, with $E_\perp$ equal to the step function $E_x(x, z_b)$ in Figure 2. What will E_x then look like at other altitudes? To answer this question an ionospheric model must be specified. Suppose that $\sigma_\parallel = i_z/E_z$ is constant above a certain altitude $z_b - h$ well above the E- and F-layers and that $\sigma_\parallel \sim \infty$ throughout the lower part of the ionosphere. This assumption enables us to get the height-integrated form of equation (3) by simply writing Σ_P and Σ_H instead of σ_P and σ_H, provided that

$$v_n \approx 0 \quad . \tag{4}$$

The Pedersen and Hall conductivities are assumed to be horizontally homogeneous.

Let us further assume that

$$\frac{\partial}{\partial y} = 0 \quad . \tag{5}$$

We now solve equation (1) with $E_x(x, z_b)$ and equations (3) through (5) as boundary conditions, recalling that

$$\operatorname{div} \bar{i} = 0 \quad . \tag{6}$$

Because the Pedersen current in this geometry has a divergence around $x = 0$, a field-aligned current flowing upward at the field reversal is obtained. Due to the finite $\sigma_\parallel$, the step in $E_x(x, z_b)$ is completely smoothed out in $E_x(x, z_b - h)$, giving a finite i_z. In flying through the field reversal at altitude $z_b + h$ we would see an $E_\perp$ profile according to $E_x(x, z_b + h)$, and at even higher altitudes the "spikes" on each side of the reversal would be even larger.

It can be seen from Figure 2 that, although the field reversal is infinitely sharp at z_b, we get a certain finite characteristic thickness of the associated field-aligned current sheet equal to 2Λ, where

$$\Lambda = \sqrt{\frac{h \cdot \Sigma_P}{\sigma_\parallel}} \quad . \tag{7}$$

That is, to get $\Lambda = 0$ we must have $\sigma_\parallel = \infty$ everywhere. This is due to the fact that $E_\perp$ has a finite amplitude at z_b (as well as all other altitudes).

It is important to notice that as $\sigma_\parallel$ decreases (increasing Λ), the potential drop along the magnetic field is reached at the expense of the transverse potential drop at low altitudes, provided that $E_\perp(z_b)$ does not increase. In Figure 2, $(\Delta V)_\parallel$ between $z_b - h$ and z_b evidently has a maximum of $\Lambda \cdot E_0$ at $x = 0$.

We further notice that the parallel electric field E_z, as well as the current density i_z, has an inverted-V profile. This is of great interest because an electric field having an upward direction on the evening side of the earth at a "regular" field reversal would be able to accelerate auroral electrons downward, producing the typical inverted-V shape of mean energy versus latitude which is seen at the field reversal at local evening [47]. This is further discussed in Section XIV.

VII. A SELF-CONSISTENT MODEL OF A STATIC $E_\parallel$

Figure 3 is a refinement of Figure 2 in that the field-aligned "resistivity," i.e., the quantity E_z/i_z, is increased only within the field-aligned current sheet. In Figure 3 $z_b = 1500$ km and $h = 500$ km. The assumed boundary value $E_x(x, z_b)$ is not a step function here but a smooth profile (see the curve labeled $z = 1500$ km). The altitude-averaged parallel electric field $\tilde{E}_z$, defined by

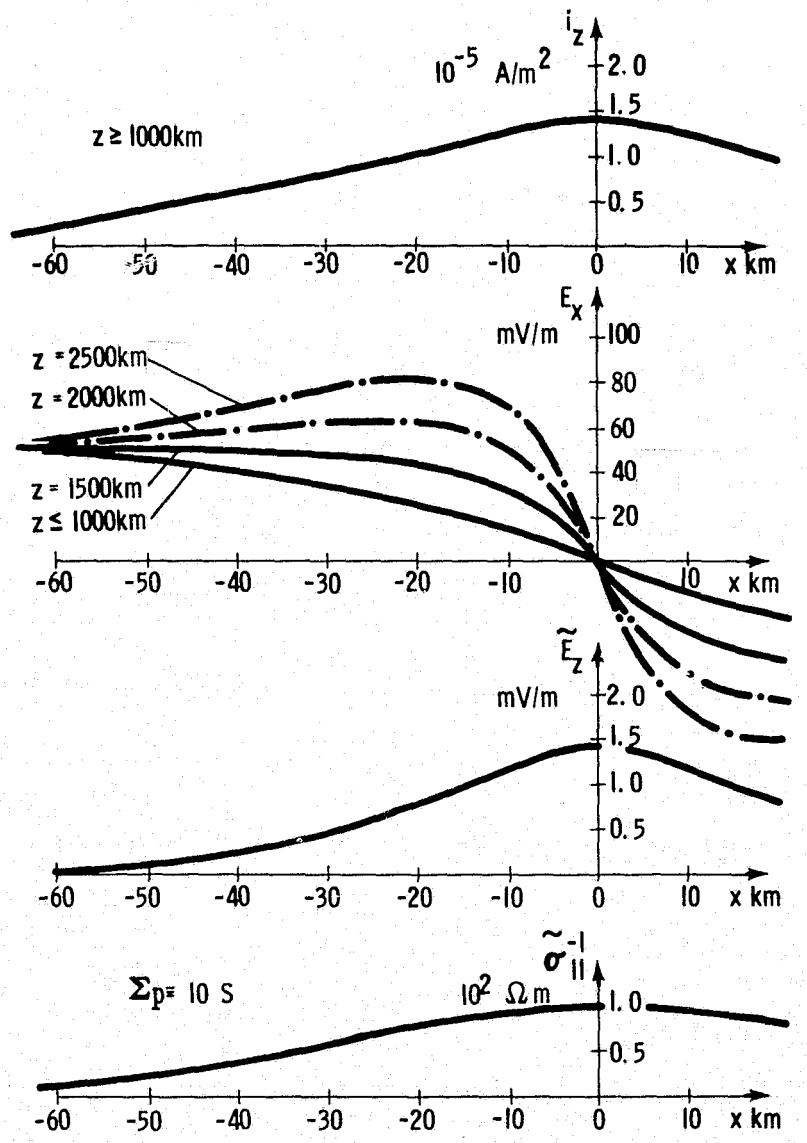

Figure 3. The analogue of Figure 2 when $E_\perp$ at z_b = 1500 km has a smooth distribution and the parallel resistivity (averaged over altitude) above $z_b - h = 1000$ km is defined by the bottom curve.

$$\tilde{E}_z(x) = \left(\frac{V(x, z_b - h) - V(x, z_b)}{h} \right) \quad ,$$

has been introduced here, as well as the altitude averaged "anomalous resistivity" $\tilde{\sigma}_{\parallel}^{-1}$; that is,

$$\tilde{\sigma}_{\parallel}^{-1} = \frac{\tilde{E}_z}{i_z}$$

(the field-aligned current is assumed divergence free above the E- and F-layers). Below $z_b - h = 1000$ km, $\tilde{\sigma}_{\parallel}^{-1}$ is assumed small (normal) in accordance with most theoretical models [10,13].

The function $\tilde{\sigma}_{\parallel}^{-1}(x)$ defined by the bottom curve in Figure 3 is simply an a priori assumption about the quantity $\tilde{E}_z/i_z$ (the peak value $10^2\ \Omega$ m is chosen to give a reasonable current density). This assumption together with equations (3) through (5) with $\Sigma_P = 10$ S has been used to solve equations (1) and (6) for $\tilde{E}_z(x)$, $i_z(x)$ and $E_x(x,z)$. The resulting distribution of $i_z(x)$, the top curve of Figure 3, then also defines $\tilde{\sigma}_{\parallel}^{-1}$ as a function of i_z. This enables us to make a better assumption concerning $\tilde{\sigma}_{\parallel}^{-1}$, recalculate i_z, etc. By this iterative process, we are evidently able to get any desired relation between $\tilde{\sigma}_{\parallel}^{-1}$ and i_z.

The dashed E_x profiles in Figure 3 show what $E_\perp$ would look like at $z = 2000$ km and 2500 km in case $\sigma_{\parallel}^{-1}$ had the same average value throughout this upper altitude region. This again illustrates the fact that the amplitude of $E_\perp$ has to be an increasing function of altitude near the reversal due to the presence of a strong $E_\parallel$. Of course, this will only be true up to a certain altitude, because $(\Delta V)_\parallel$ is finite. Above this altitude, $E_\parallel$ is expected to be small (in general) and the amplitude of $E_\perp$ to be decreasing with increasing altitude, because of the diverging magnetic field lines [see the scaling factor in equation (2c)].

Despite the obvious difference between the two models, the quantity Λ according to equation (7) again gives a good measure of the latitudinal width of the $\tilde{E}_z$ profile in Figure 3 with the peak value $10^2\ \Omega$ m inserted for $\sigma_{\parallel}^{-1}$. Also, the maximum potential drop between $z = 1000$ km and $z = 1500$ km is again at least of the same order of magnitude as $\Lambda \cdot E_0$.

In Figure 3, Σ_P is still horizontally homogeneous, but an assumed profile $\Sigma_P(x)$ can easily be introduced in the model to give a modified i_z and E_z, which then helps in making a better assumption concerning $\Sigma_P(x)$. This is provided that we specify the energy of the electrons before they are accelerated by $(\Delta V)_{\parallel} = h \cdot \tilde{E}_z$. In this way the model can be made self-consistent. The main effect of a locally enhanced $\Sigma_P(x)$ at the base of a field-aligned current sheet, when $\sigma_{\parallel}$ is small and $E_{\perp}$ is given at a certain high altitude, is just a corresponding local reduction of $E_{\perp}$ at low altitudes, as has been shown in a previous paper [48] (see also Section XIV). The local increase of Σ_P will certainly have a feedback effect on the magnetospheric "dynamo," which this simple model cannot account for, however. Neither can this model in an adequate manner account for the auroral electrojet, which requires a three-dimensional geometry.

It may be noted that if this simple model is extended to very high altitudes [utilizing equation (2c), for instance], we can no longer neglect the (unknown) transverse current that is feeding the current loop (the dynamo current).

VIII. ANOMALOUS RESISTIVITY AND THE MAGNETIC MIRRORING

Suppose for a moment that we can neglect the mirroring effect of the geomagnetic field where $E_{\parallel}$ is large (consider Figure 1b). It is quite obvious that an electron that has gained the energy $e \cdot (V_1 - V_2)$ by falling from z_2 to z_1 at the same time has made its maximum possible contribution to a short-circuiting current. That is, a freely falling electron in this case represents an extremely high conductivity per particle. Thus, for the potential jump $V_1 - V_2$ to be maintained, the number flux of these electrons has to be limited in one way or another.

In the theory of anomalous resistivity [36] it is assumed that there is a sufficiently dense population of thermal electrons (and ions) to short-circuit any $E_{\parallel}$ in the classical sense; but due to the high relative drift velocity between electrons and ions, plasma wave instabilities are generated that transform the laminar flow into random (thermal) particle motion, thereby limiting the electron drift velocity.

When this concept is being applied to the auroral problem, it is generally assumed that the thermal particles are cold electrons and ions of ionospheric (topside) origin. This assumption is usually made as a mere basis for quantitative evaluation of the instability criteria of different wave modes, and it is anticipated that the saturating plasma wave instabilities will be associated with conditions different from the initial state [13]. In this theory, at least with respect to the nonsaturated state, the electrons having a parallel energy of the same order as $e(V_1 - V_2)$ then have to be a minority group of either "runaway" electrons or hot magnetospheric electrons passing by, unaffected by the wave field. Because these relatively dilute electrons have a much higher parallel velocity, they may possibly be capable of carrying a major portion of $i_{\parallel}$ in accordance with auroral particle observations [20, 22, 33]. However, the theory is based on a certain minimum drift velocity of the thermal electrons which together with the assumed plasma density does require a minimum parallel current density being carried by thermal electrons, $i_{\parallel}$ (thermal). Consequently, a certain minimum fraction of the electrostatic energy (provided by an external dynamo) being released per unit area per second, $i_{\parallel} \cdot (V_1 - V_2)$, has to be converted to random motion, that is into heat [40]. With at least $i_{\parallel}$ (thermal) $\sim 10^{-5}$ A/m^2 [13] $V_1 - V_2 = 5$ kV, $z_2 - z_1 = 10^4$ km (see Fig. 1b) and a density of thermal electrons and ions of 10^9 m^{-3}, we get a heating rate of 30 eV per second per thermal particle, to be compared with the original thermal energy of less than 1 eV per particle [40]. A certain fraction of this energy may possibly be radiated away by plasma waves, but there is no theory disproving that the auroral plasma temperature would be drastically increased (in the theory by Buneman this heating is a desired effect [49]). We notice here that as the temperature is increased, a higher $i_{\parallel}$ is required to maintain the plasma drift instabilities, which means that we immediately get into conflict with the discussion in Section V.

The theory of double layers, however, does not suffer from this heating dilemma according to Block [10, 40] because the particle motion is basically laminar at a double layer. The theory of double layers will not be discussed in this report, however. The reader is referred to the papers by Block [10, 40] mentioned previously, as well as the papers by Swift [11] and Kan [35] on oblique double layers (electrostatic shocks).

Apart from the heating problem there is also a problem of plasma depletion connected with any theory that requires a strong (upward) $i_{\parallel}$ to be carried by a cold background plasma of ionospheric origin. Suppose, for instance, that the density n of cold electrons at an altitude of 3000 km is 10^2 cm^{-3} [50] and that n decreases proportionally to B upwards, giving $n \sim 0.1$ to 1 cm^{-3} at the equatorial point of the magnetic field line. This probably gives an overestimation of the cold-plasma content in the magnetic flux tube since mass spectrometer data [51] frequently show a total ion density of only 0.1 cm^{-3} in the plasma sheet. An upward field-aligned current with $i_{\parallel} \sim 10^{-5}$ A/m^2 at topside altitudes, carried by downward-moving electrons, would evidently deplete all available cold electrons above 3000 km altitude within approximately 2 to 5 min (provided that the current sheet does not have a persistent horizontal motion relative to the plasma). Within a few more minutes even the topside ionosphere would suffer a strong depletion. If $i_{\parallel}$ as high as 10^{-4} A/m^2 is required by the theory, the depletion problem becomes extremely critical. We cannot really expect the cold plasma to be supplied from adjacent flux tubes by convection, as the convection is generally found to be along auroral arcs [34, 45,47]. At $i_{\parallel}$ as high as 10^{-5} to 10^{-4} A/m^2, the contribution from upward-moving protons can be neglected, even though these can, in principle, be continuously supplied by the topside ionosphere. In fact, this proton current cannot be stronger than allowed by the escape flux (10^{-7} to 10^{-6} A/m^2) [15,16]; that is, it is "temperature-limited." The "spacecharge-limited" proton current is even many orders of magnitude weaker [52]. Consequently, the only available carriers of a persistently intense upward $i_{\parallel}$ are the hot electrons from the outer magnetosphere.

Let us now take into account the magnetic mirroring effect within the acceleration region. The previous statement about the high "conductivity" of "freely falling" electrons no longer holds true because the magnetic mirror tends to obstruct the parallel current by deviating the parallel motion of the electron into transverse motion (without changing the particle energy). Apparently, this may even constitute the only necessary mechanism for obstructing $i_{\parallel}$ and maintaining a large total potential drop along the geomagnetic field lines, provided that the density of the charge carriers is not too large. In view of the fact that an upward current (downgoing electrons) may have to be carried mainly by electrons from the dilute and hot plasma in the outer magnetosphere, this mechanism seems to have been somewhat overlooked over the years. To lower by means of $E_{\parallel}$, the mirror point of an electron having a magnetic moment $\mu = mv_{\perp}^2/2B$ from a point where $B = B_1$ and $v = v_1$ to a point where $B = B_2$, the necessary $(\Delta V)_{\parallel}$ is given by

$$e(\Delta V)_{\parallel} = \mu(B_2 - B_1) = \frac{m}{2} v_1^2 \left(\frac{B_2}{B_1} - 1\right) \quad . \tag{8}$$

Suppose the flux is isotropic in the outer magnetosphere and the average electron energy is K in the absence of a $(\Delta V)_{\parallel}$. For the precipitation flux density at ionospheric altitudes to increase by, for instance, a factor of four, all electrons mirroring below an altitude of approximately 0.6 earth radii have to be lowered to the bottom of the ionosphere. From equation (8) it can be seen that the required $e(\Delta V)_{\parallel}$ is approximately 3K. If the source plasma (e.g., the plasma sheet) has a density of 0.5 cm^{-3} [51] and an average energy of 1 keV [4], for instance, $i_{\parallel}$ is thus still only approximately 6×10^{-6} A/m^2 at ionospheric altitudes with $(\Delta V)_{\parallel} \approx 3$ kV. This might seem to point towards a strong reluctance among the magnetospheric (e.g., plasma sheet) electrons to "short-circuiting" a parallel electric field. We note that the $(\Delta V)_{\parallel}$ required to drive a certain high $i_{\parallel}$ will increase with increasing temperature (at constant density) of the hot source plasma, as long as the temperature is not too high.

Recently calculations of $i_{\parallel} - (\Delta V)_{\parallel}$ relations in kinetic collision-free models under steady-state conditions have been made by Knight [14] and Lemaire and Scherer [15,16]. These authors have used slightly different models, but they get fully compatible solutions in one particular respect. That is, with reasonable ionosphere-plasma sheet parameters, an upward $i_{\parallel}$ of the order of 10^{-5} A/m^2 has to be carried mainly by precipitating electrons (rather than upflowing ions) and may readily require a total $(\Delta V)_{\parallel}$ of 1 to 10 kV. See Figure 3, p. 745, in the paper [14] by Knight and Figure 1, p. 1486, in the later paper [16] by Lemaire and Scherer (note that 5×10^{-6} A/m^2 should evidently be only 1.5×10^{-6} A/m^2 on the right hand vertical scale in this latter figure). Knight has neglected the ionospheric ion contribution to $i_{\parallel}$, while this is included by Lemaire and Scherer, but the difference is obviously insignificant when $i_{\parallel} \gtrsim 10^{-5}$ A/m^2.

Unfortunately, the model by Knight provides only the total voltage $(\Delta V)_{\parallel}$ while $E_{\parallel}$ remains undetermined ($E_{\parallel}$ is assumed not to change sign along the magnetic field). The model by Lemaire and Scherer does provide $E_{\parallel}$ numerically, but the case of a strong upward $E_{\parallel}$ is not explicitly shown.

It must be remembered that these two models rely upon the outer magnetosphere (the plasma sheet) providing a steady supply of isotropic electrons. The need for a high $(\Delta V)_{\parallel}$ will evidently be larger if the magnetospheric particle source is depleted of electrons with small pitch angles.

IX. THE SPATIAL DISTRIBUTION OF $E_{\parallel}$ AND THE RAY STRUCTURE OF AURORAS

In view of Section V, it may seem to be difficult to reconcile auroral fine structures like visible auroral rays (and very thin current sheets) with a particle acceleration due to a large $(\Delta V)_{\parallel}$. This is particularly true of current-driven instabilities as we then would expect the cross-sectional dimensions of a current sheet or current beam to directly map the transverse dimensions of the $(\Delta V)_{\parallel}$ -region, cf. equation (7). This may thus strongly favor the magnetic mirroring as the actual current obstructing mechanism, as will be seen.

It is straightforward to show that a low-density plasma, like the magnetospheric plasma in a magnetic mirror field, may well permit a large $E_{\parallel}$ without any $i_{\parallel}$ flowing [37-39]. Actually, with $i_{\parallel} = 0$ the parallel electric field is zero only if the electrons and ions have identically the same pitch-angle distributions [38]. From this we may be led to the following hypothetic model.

By the magnetic mirroring of incoming electrons, a large $(\Delta V)_{\parallel}$ may be maintained within a region that has large dimensions along, as well as transverse to, the magnetic field. The direction of $(\Delta V)_{\parallel}$ is to force electrons downward (see Section XIII for the driving dynamo), but net field-aligned currents may be flowing preferably in thin field-aligned subregions of the region where $E_{\parallel}$ is large.

This model helps to satisfy Section V, and we may even permit thin auroral rays to be energized by $(\Delta V)_{\parallel}$. What remains is a mechanism that locally reduces the magnetic mirroring effect on electrons. The solution of this may well be wave-particle interactions. There are a number of plasma wave modes that resonate with the gyromotion of electrons [2,6,53,54], and we may picture a situation where the gyro energy is being drained by the waves,

while at the same time the large-scale $E_{||}$ is feeding energy into the longitudinal motion (and the magnetic field deviating parallel energy into transverse). As will be seen in the next section, this may also provide a mechanism for confinement in velocity space to small pitch angles.

The distribution along the magnetic field of $E_{||}$ in a magnetic mirror configuration is a separate problem that has been treated in certain aspects by, among others, Persson [39]. Persson finds, for example, that in a stationary state with no field-aligned currents and with "almost isotropic" distributions for electrons and ions the parallel electric field is given by

$$E_{||} \propto \text{grad}_{||} B \quad . \tag{9a}$$

This particular form of $E_{||}$ will be used in Sections X and XII for some illustrative calculations. Although equation (9a) was derived by Persson in a case with no net field-aligned currents, it will be seen in the next section to be a very basic distribution applicable also to cases with a large $i_{||}$ flowing. Even though equation (9a) may not be exactly fulfilled in a case as complex as the auroral case, it may be expected to be a reasonable first order approximation in many cases because it does reflect the basic balance between the electric and magnetic forces. An $E_{||}$ according to equation (9a) apparently requires a dilute plasma of predominantly energetic particles, which means that this kind of electric field at a given moment may be found only above a certain altitude, where the cold particles are depleted, whereas $E_{||}$ may be "screened out" at lower altitudes by the cold plasma still remaining there. At a moment when equation (9a) is valid down to altitudes of only a few thousand km, most of the associated $(\Delta V)_{||}$ will evidently fall below an altitude of one earth radius above the ionosphere.

X. THE COLLIMATION OF ELECTRON BURSTS

It is quite obvious that the combined action of the magnetic mirror and a parallel electric field makes the pitch-angle distribution at a given altitude a rather ambiguous indicator of the acceleration process, in particular when rapid

fluctuations occur. However, a few basic features may be expected from a given electric field distribution [e.g. equation (9a)]. Let us introduce the length coordinate s along the magnetic field. Equation (9a) may then be written

$$E_{\parallel} = -\kappa \frac{dB}{ds} \tag{9b}$$

where κ is a positive constant (constant along a certain field line). The equation of motion along the magnetic field for an electron is then

$$m_e \frac{dv_{\parallel}}{dt} = (e\kappa - \mu) \frac{dB}{ds} \tag{10}$$

where $\mu = m_e v_{\perp}^2/2B$ is the magnetic moment. In going from point 1 where $B = B_1$ to a point 2 where $B = B_2 > B_1$, an electron increases its total kinetic energy according to

$$\frac{m_e}{2}(v_2^2 - v_1^2) = e(V_2 - V_1) = e\kappa\,(B_2 - B_1) \quad . \tag{11}$$

As long as μ is constant, we then have

$$\frac{v_{\perp_2}^2 - v_{\perp_1}^2}{v_2^2 - v_1^2} = \frac{\mu}{e\kappa} \quad ; \tag{12a}$$

that is, if $B_2 >> B_1$ $(v_{\perp_2} >> v_{\perp_1})$,

$$\sin^2 \alpha_2 = \frac{v_{\perp_2}^2}{v_2^2} \lesssim \frac{\mu}{e\kappa} \quad . \tag{12b}$$

The pitch angle α tends to stay smaller than or equal to a certain constant, defined by the magnetic moment of the electron. With a given energy at point 1 the electron with the smaller α will leave the electron with the larger α behind. This effect will evidently be extremely pronounced with an $E_{\parallel}$ according to equation (9a), because $v_{\parallel}$ of an electron with $\mu < e\kappa$ will increase with increasing distance along the trajectory [cf. equation (10)], and $v_{\parallel}$ will increase more the smaller μ is. If a cloud of electrons is injected at point 1 having electrons with $\mu < e\kappa$, it is expected to show up as a burst of electrons with very small pitch angles at point 2, in agreement with auroral observations [1,20].

How do we envisage a "particle injection" at point 1? Again the resonant wave-particle interaction may be a convenient tool. Suppose that a gyro-resonant plasma-wave instability is "switched on" at point 1. This may drain the transverse kinetic energy from a large number of electrons near point 1, forcing them into the small μ region where $\mu < e\kappa$; this, in turn, will cause a collimated beam of electrons to appear at low altitude. From this model, it is expected that an auroral ray will often appear as a collimated burst when observed by a rocket flying through an auroral display.

These results will evidently be largely true with any (upward) $E_{\parallel}$ that is distributed along $\bar{B}$ but mainly concentrated to the region of strong magnetic field. However, as can be seen from equations (9b) through (12b), the distribution according to equation (9a) is in a certain sense unique. Although $E_{\parallel}$ is subject to the quasi-neutrality of the plasma, it is basically due to an externally applied $(\Delta V)_{\parallel}$ (Section XIII); that is, within the limitations of the quasi-neutrality of the actual particle population, the electric field will adjust to the magnetic-field gradient to make $i_{\parallel}$ as large as possible. From this point of view, equation (9a) is evidently a very efficient distribution, because it tends to make the pitch angle a constant of the motion for electrons with $mv^2/2 \lesssim e\kappa B$. Hence, if $E_{\parallel}$, with a given total $(\Delta V)_{\parallel}$, is relatively more concentrated to low altitudes than equation (9a), the current will be smaller, in general. If, however, $E_{\parallel}$ is relatively more concentrated to high altitudes than equation (9a), it does give the same current as equation (9a); but in this case the high-altitude portion of $(\Delta V)_{\parallel}$ is apparently larger than needed to carry the present current, at least if the electron distribution is isotropic (or field-aligned). This will be investigated further (see also Section XII).

XI. COMMENTS ON THE ELECTRON ENERGY SPECTRUM

Consider equation (11). If the initial energy at point 1 is small compared to $e(V_2 - V_1)$, only a small total amount of kinetic (gyro) energy has to be removed by wave-particle interactions at point 1 to create a large enhancement of the electron energy flux at point 2. However, any electron that is being mirrored at a point close to point 2, between points 1 and 2, can lose all its gyroenergy and arrive at point 2 virtually without any energy. That is, as long as we do not specify in detail the process of wave-particle interactions, there is a wide range of possible precipitation modes within the present model.

There may also be many different wave-particle interactions connected mainly with the parallel motion of the electrons [53]. The precipitating electrons will evidently be streaming past the upward flowing (accelerating) positive ions from the ionosphere, which may lead to favorable conditions for the two-stream instability. These kinds of wave-particle interactions, in particular, may seem likely to generate a component of the precipitating electrons having a strongly degraded energy, as compared with the "free-fall" component. More generally, wave-particle interactions may cause the electrons to diffuse in velocity space, preferably towards smaller velocities, although some precipitating electrons may gain kinetic energy in this way.

It may seem intuitively reasonable that a spatially widely extended plasma is particularly susceptible to instabilities in velocity space because it allows unstable traveling waves to grow for extended periods of time [55]. A spatially strongly limited plasma, however, may seem to be very stable against this kind of wave growth, as the wave packets may generally pass out of the plasma before they reach a large amplitude, or the wave length may be relatively too large to allow an efficient wave growth. In fact, both artificial generation of thin "auroral" electron beams [55] and theoretical investigations [56] do indicate that a thin structure of precipitating electrons is very stable to energy degradation by wave-particle interaction.

It is tempting to apply these ideas to the present model. Within the latitudinally (and longitudinally) extended region of high $(\Delta V)_{\parallel}$, the precipitating electrons may get somewhat degraded in energy, for instance by interacting with the upflowing ionospheric ions. Because the backscattered and numerous secondary electrons will evidently be reflected downward by $(\Delta V)_{\parallel}$ [57], the total energy spectrum of precipitating electrons at low altitudes may thus possibly look fairly smooth even with a high $(\Delta V)_{\parallel}$ present. However, gyroresonant wave-particle interactions may locally increase the number of electrons

with $\mu < e\kappa$ at high altitudes. When continuing downward, these electrons will form a thin structure of increased number density [consider $nv_{||} \sim B$ and equation (11)] that may thus become stable against further energy degradation, leading to a bright auroral form and a pronounced "monoenergetic" peak in the energy spectrum [1, 17]. That is, in cases with thin auroral forms, one might expect to find a much more pronounced monoenergetic peak inside the auroral form than outside, even though $(\Delta V)_{||}$ may be high within a much broader region. This will be discussed further in Section XIV.

XII. A GENERALIZED "LOSS-CONE" FOR THE ELECTRONS

As an electron with a large magnetic moment will become mirrored, there may often be a tendency towards negative charge-accumulation on a closed field line with upward currents. This may tend to quench the magnetospheric dynamo current (see Section XIII), leading to a loss-cone distribution of electrons with $\mu < e\kappa$ [equation (10)]. Evidently, this loss-cone will be larger for electrons having a smaller total energy than for the more energetic electrons. That is, given a point on a closed magnetic field line, where the magnetic field strength is B, the half-angle α_{1e} of the local loss-cone is defined by

$$\sin^2 \alpha_{1e} = \frac{B}{B_{max}} + \frac{e\kappa B}{\frac{m_e v^2}{2}} \left(1 - \frac{B}{B_{max}}\right) \qquad (13)$$

where B_{max} is the magnetic field strength at the altitude of the low ionosphere (it is assumed for simplicity that $E_{||}$ penetrates to low altitudes). No electrons with $m_e v^2/2 \leq e\kappa B$ will remain. Equation (13) follows from equation (11) and the constancy of μ.

The corresponding equation for the proton loss-cone is analogous to equation (13) with the plus sign changed to a minus sign. This is then applicable to all protons with $m_p v^2/2 \geq e\kappa (B_{max} - B)$. Protons with lower energies will have no loss-cone.

If the electric field is increased, that is, if κ is increased to $\kappa' > \kappa$, electrons will start precipitating again with pitch angles given by

$$\frac{\kappa}{\kappa'} \leq \sin^2\alpha \leq 1 \tag{14}$$

at the altitude of the low ionosphere. The half-angle of the apparent loss-cone at ionospheric altitudes will thus rapidly decrease from 90° to the lower limit determined by equation (14) and then slowly increase again. Provided that the electric field has a negligible growth time, the time scale of the initial decrease of this loss-cone will be roughly defined by the time it takes an electron with a low initial energy to fall from an altitude of one earth radius [equation (9a)], that is typically of the order of a second or less. The time scale of the subsequent increase of the loss-cone, however, will be determined by the travel time from the outer magnetosphere of the lowest energy electrons, which may be several tens of seconds (with initial energies of the order of 100 eV or less).

An interesting special case of equation (14) is $\kappa = 0$. More generally, let us suppose that $\kappa' >> \kappa$ and that the average electron energy prior to the increase of $E_{||}$ is much smaller than $e\kappa' B_{max}$, that is, much smaller than the energy of the subsequently precipitating electrons. It then follows that the more energetic electrons arriving at the low ionosphere, on the average, are more "field-aligned" than the less energetic.

The reason for this is twofold: after the electric field is "turned on," a given electron from the precipitating population will reach the low ionosphere at a smaller pitch angle and a higher energy if it is initially at a higher altitude. This is easily seen from equation (11) and the constancy of μ (even if the time change of $E_{||}$ at some point is rapid compared with the local electron gyro frequency, it does not directly influence $v_\perp$ and it gives only a negligible and temporary change in $\bar{B}$). Furthermore, as a consequence of the velocity dispersion (due to different pitch angles at given initial energy), an electron from a higher altitude (higher final energy) will reach the low ionosphere with a certain pitch angle at the same time as an electron from a lower altitude (lower final energy) with a larger pitch angle. This apparent relation between energy and pitch angle will be most pronounced during the initial phase of the precipitation event, while during the later phase of the loss-cone recovery the precipitation will evidently approach monoenergy. We have not invoked any wave-particle interactions in this section, and such nonadiabatic processes might be expected to modify these results to some extent. (See the discussion of these results in Section XIV.)

It may be noted that otherwise isotropic electron and proton distributions remaining after these loss-cones have been emptied are consistent with equation (9a); that is, the electric field will, in principle, be "frozen in" in the remaining (quasi-neutral) distributions, even if the external dynamo is "turned off." In fact, the remaining pitch-angle distributions at each energy are evidently equivalent to the monoenergetic and "almost isotropic" distributions found by Persson [39] to give equation (9a). However, when the dynamo is turned off, there is nothing that prevents the ionosphere from decreasing in potential when the ionospheric ions flow upwards; consequently, the upward $E_{\parallel}$ will be rapidly eliminated.

XIII. THE MAGNETOSPHERIC DYNAMO

The current configuration of Figures 2 and 3 may correspond to current loops of those sketched in Figure 4. The view of Figure 4 is in the direction towards the sun. Figures 2 and 3 may be thought of as pictures of a small region around point D. In this particular case Pedersen currents are flowing in towards the upward current sheet from the north and south side. The poleward downward current may flow either from A' to D' or from W down the dotted line (that is, close to A-D), or probably both ways. This symmetric situation may not be the typical case in reality, where we may even have multiple field-aligned current sheets [58].

A magnetospheric dynamo driving a current down to the ionosphere and back up is basically a continuously progressing charge separation in the outer magnetosphere driven by, e.g., inertia forces on the charge particles. The dashed current loop in Figure 4, e.g., may be accomplished by the ionospheric drag (in a hydromagnetic sense) on the solar wind flow via open (merged) magnetic field lines. This case is a "voltage-generator," where the charge separation between A and A' is produced, basically, by solar wind protons displacing their gyrocenters in a direction opposite to (and the electrons in the same direction as) $\bar{E}_{\perp}$, when entering a region of reduced $E_{\perp}$ (reduced $E \times B$ drift) [59]. That is, kinetic energy associated with $E \times B$ drifting solar wind protons (and electrons) is converted into electrostatic energy. If the solid current loop in Figure 4 is on closed magnetic field lines, the driving charge separation between A and B may, e.g., be due to gradient-B drift of energetic particles across inhomogeneities in their density and temperature distributions, as in the model by Jaggi and Wolf [60]. This case is more like a "current-generator," although not in a strict sense. Indirectly, the solar wind is the driving agent

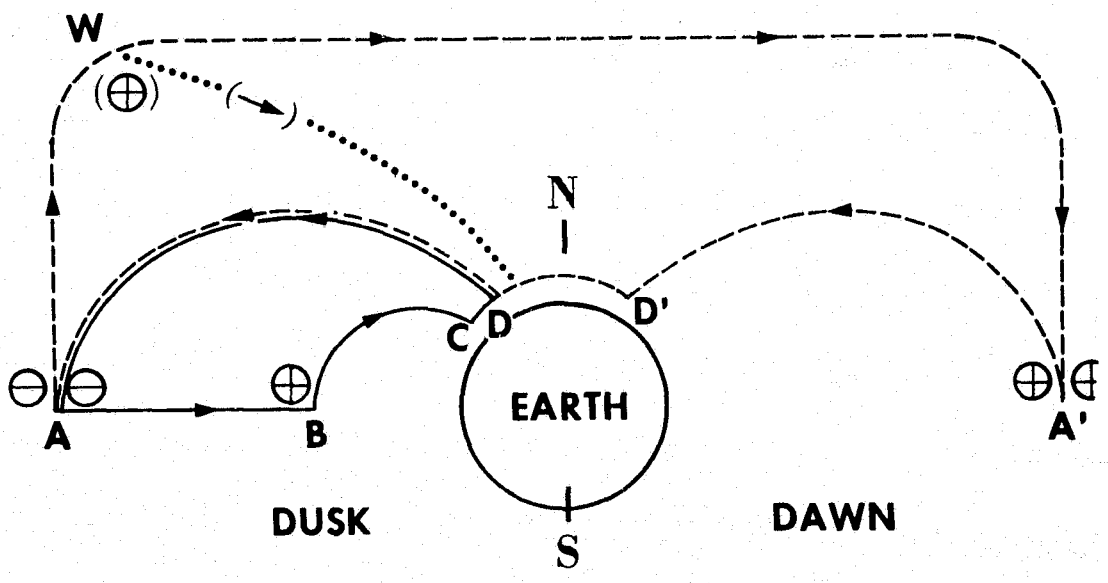

Figure 4. A possible configuration of a magnetosphere-ionosphere current system (projected onto the dawn-dusk plane) (the current paths B-C, D-A and A'-D' as well as the dotted path are parallel to the magnetic field, while the remaining current paths are in the transverse direction. The dashed current path A-W-A' is within the solar wind.)

in this case, too, since the solar wind flow is what causes the internal magnetospheric convection (sunward). This convection carries the charged particles into the Earth's magnetic field, leading to betatron and Fermi acceleration of the particles [37].

Dynamo models presented so far, like that by Jaggi and Wolf [60], rely upon the assumption of zero parallel electric fields. In view of our arguments in Section VIII, this seems to be a highly dubious assumption, at least for upward currents. On the contrary, it is suggested that the negative space charge (electrons) at A is not readily discharged to D because of the magnetic mirroring of the major charge carriers, which are downward moving electrons [equation (8)] [14]. The upward positive-ion flux (mostly protons) from the ionosphere will be roughly "temperature-limited" by the natural thermal outflux of topside ions, giving a contribution to $i_{\parallel}$ on the order of only 10^{-7} to 10^{-6} A/m^2 [16]. We do not reject double layers or anomalous resistivity as being involved in the current obstruction, but we are emphasizing the magnetic mirroring as the presumable basic cause of a large $(\Delta V)_{\parallel}$.

Because the conductivity along D-A is finite, the potential difference between A and B does not simply map onto D-C but is partly taken up by A-D, leading to an $E_{||}$ according to equation (9a), for instance. Even with a constant potential between A and B, the $(\Delta V)_{||}$ between A and D may still increase at the expense of the potential between D and C (see Section VI). In accordance with the present model, the gyroresonant plasma-wave instabilities are expected to release local bursts (rays) of electrons that, consequently, decrease the effective "resistance" of the (wide) current path D-A, but these may not be sufficiently intense to short-circuit $(\Delta V)_{||}$.

The downward current B-C, however, is expected to flow without any significant $(\Delta V)_{||}$, in general, because even a very small downward $E_{||}$ will release a high escape flux of ionospheric (topside) electrons [14-16].

The magnetic energy stored in the current loops is also capable of modulating the acceleration conditions along A-D. This will not be discussed in a strict manner in this report. Only one very brief sketch will be given in the next section of some conceivable consequences that may be related to pulsating auroras and certain recent particle observations in the outer magnetosphere.

XIV. COMPARISON WITH OBSERVATIONS

As already mentioned in Sections III and VI, the convection electric field in the altitude range 500 to 2500 km has been extensively explored by polar orbiting satellites [26,47,61-64]. It is found that the convection is generally antisunward over the polar caps down to the poleward edge of the auroral ovals (at 70° to 80° magnetic latitude) and sunward between this region and the plasmasphere (except for stagnation lines near noon and midnight). The transition between antisunward and sunward convection is generally observed as a fairly sharp reversal of $E_{\perp}$, and adjacent to the main reversal the $E_{\perp}$-field is often strongly fluctuating (as seen by the moving spacecraft) with pronounced peaks. It has further been established [23,25,47,65] that on the evening side this field reversal is frequently associated with bands of intense inverted-V events, that is, field-aligned sheets (probably east-west oriented) of precipitating electrons characterized by an inverted-V profile of mean energy versus latitude, as seen by a satellite crossing the sheet. From Sections VI and VII such an inverted-V event associated with the field-reversal on the evening side would be expected, where the associated $i_{||}$ is upward, in contrast with the morning side (Fig. 4).

The basic results of Sections VI and VII require only a pronounced horizontal gradient in $E_\perp$; that is, inverted-V events may as well be associated with the irregularities in $E_\perp$ adjacent to the main reversal, in accordance with the observations. The real situation, however, may be strongly complicated by horizontal gradients in Σ_P (and Σ_H), in particular when the precipitation structure is moving. A further complication is introduced by the (generally) unknown neutral gas velocity, which may also slightly displace the inverted-V structure relative to the observed inhomogeneity in $E_\perp$ [48]. That is, some ambiguity might be expected when interpreting the observations. As long as Pedersen currents are the major source of the upward $i_\parallel$ and the gradient in $E_\perp$ is mainly responsible for $i_\parallel$, the $E_\perp$-gradient has to be in a certain direction. That is, more $E_\perp$-field lines have to point towards the upward current sheet than away from it. We thus interpret the occasional observation of inverted-V events in the field-reversal region in the morning sector as due to the presence of a $\text{grad}_\perp E_\perp$ with the "right" sign close to the main reversal. This seems to be in full agreement with data from the Ion Drift Meter [66] on Atmosphere Explorer C, according to Burch.[1]

We note from the simple models in Sections VI and VII that the inverted-V shape is the simplest possible latitudinal distribution of $(\Delta V)_\parallel$ that can be expected at an upward field-aligned current sheet when the parallel "conductivity" is finite.

The inverted-V events, in general, are fairly thick sheets of precipitation, typically 100 to 250 km [65], which obviously is in full agreement with Section V [equation (2b)]. It is even observed that in the direction from early to late local evening the inverted-V precipitation bands grow more energetic *and* wider [47], which is in qualitative agreement with Section V under the assumption that $E_\perp$ at large distances from the Earth (the dynamo field) stays fairly constant (cf. equation (2c); cf. also equation (7) and the two subsequent paragraphs in Section VI); note that a decreased "$\sigma_\parallel$" may be due to an increased temperature of the hot source plasma (cf. equation (8) and the subsequent paragraph in Section VIII).

Often very pronounced peaks with opposite signs in $E_\perp$ are observed at each border of an inverted-V event. According to Burch (private communication),

1. Private communication.

the ion drift data from Atmosphere Explorer C [66] show such pronounced peaks to be in the "right" sense in all cases examined, that is, with $E_\perp$ pointing toward the center of the inverted-V event. Besides, Burch found one pair of opposite $E_\perp$ peaks where $E_\perp$ pointed outwards, and this single case was seen to be associated with a three orders of magnitude dropout in the electron precipitation flux between the $E_\perp$ peaks as compared with the surrounding flux. Even if the satellite is observing the uppermost $E_\perp$ curve in Figure 3, e.g., a large fraction of the observed $E_\perp$ is evidently due to the low-altitude field needed to carry the Pedersen currents towards the upward current sheet. That is, we do not expect the integral of $E_\perp$ along the satellite trajectory to be a true measure of the $(\Delta V)_\parallel$ below the satellite. The "asymptotic" $E_\perp$-field on both sides of the reversal in Figures 2 and 3 in reality may well go to zero within a short distance from the reversal, associated with the downward $i_\parallel$-sheets (upflowing ionospheric electrons) as sketched in Figure 5. This means that the satellite may at times observe two apparent "spikes" in $E_\perp$ even if it is actually observing only the low-altitude $E_\perp$.

Observations indicate that $E_\perp$ is reduced within auroral arcs due to the enhanced Σ_P and Σ_H [44-46]. This is in full formal agreement with a large $(\Delta V)_\parallel$, as shown in an earlier paper [48], and may be qualitatively understood as the low altitude $E_\perp$ adjusting to gradients in Σ_P to avoid a too high $i_\parallel$, that is, to avoid a too high $(\Delta V)_\parallel/\Delta x$ according to equation (2b). This is provided that $E_\perp$ at high altitudes (the dynamo field) is not allowed to increase. This is also illustrated in Figure 5, where the low-altitude $E_\perp$ is "shorted out" within the upward current sheet (precipitating electrons).

As mentioned in Section IV, observations often indicate that $i_\parallel$ as inferred from magnetic measurements is equal to or even larger than the current density inferred from the detected precipitation [19, 20, 28-34]. We found (Section IV) that this is seemingly the same as keeping the ionosphere at a higher potential than the adjacent magnetosphere. Obviously, this is easily understood in terms of a large $(\Delta V)_\parallel$ in a direction to accelerate electrons downwards (along A-D in Figure 4). These comments apply in principle to any large $(\Delta V)_\parallel$. Now let us consider some observations that may favor the combined model of magnetic mirroring and plasma waves.

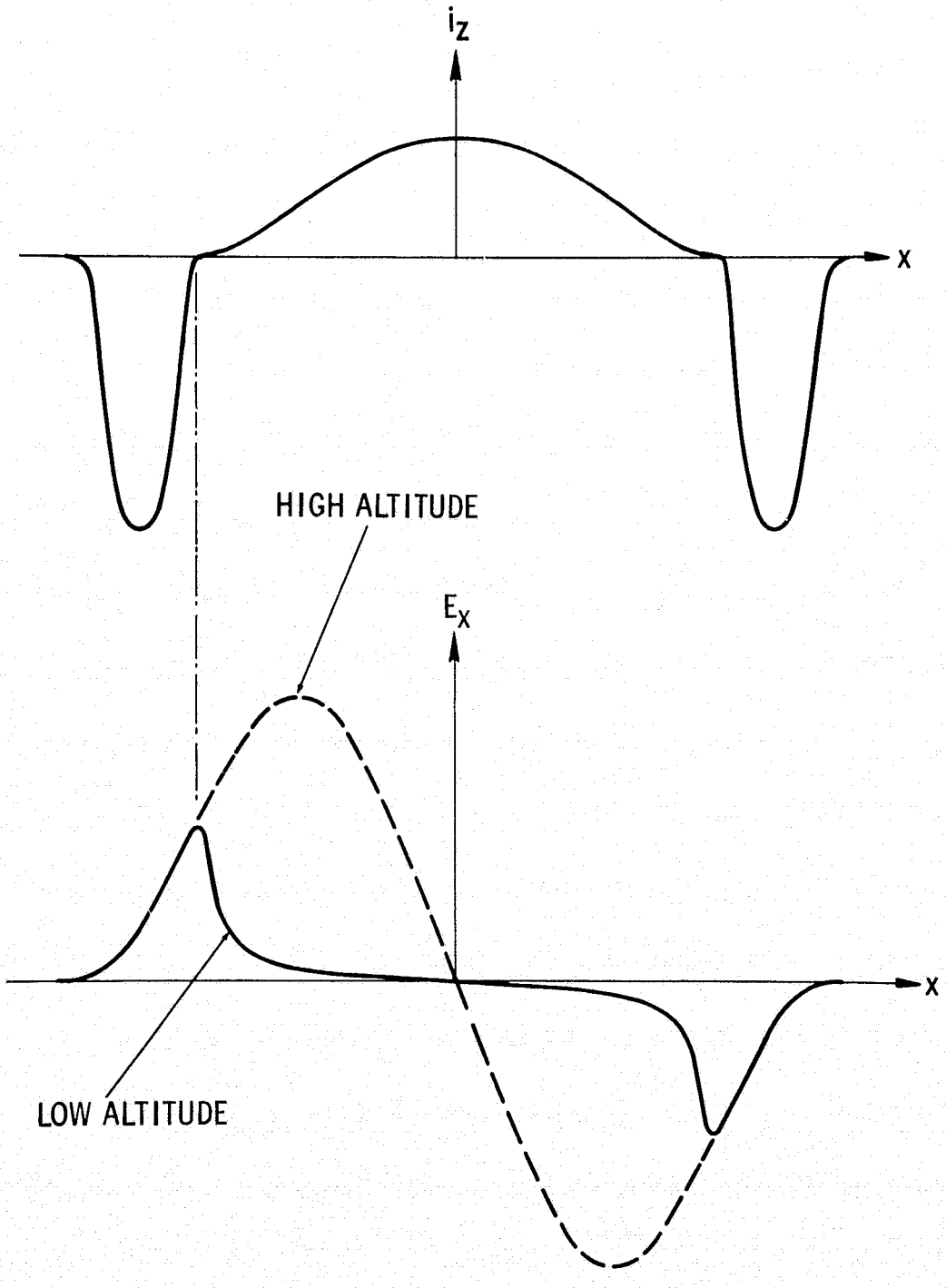

Figure 5. A sketch of a case where the downward currents flow immediately outside of the upward current sheet (precipitating electrons) (only the upward current is assumed associated with a small $\sigma_{||}$. The low-altitude E_x is "shorted out" within the precipitation structure, as a result of the enhanced ionization.).

We recall that the inverted-V structures are often fairly wide in latitude and, hence, often associated with average $i_{||} \sim 10^{-6}$ A/m^2 (or less) at ionospheric altitudes [23,25,26,47,61-65]. This evidently places a severe restriction on a current-driven instability being the cause of $(\Delta V)_{||}$. However, the interpretation in terms of magnetic mirroring is, in principle, not affected since $(\Delta V)_{||}$ in this case will be determined by the overall supply of electrons with small magnetic moments provided the outflux of ionospheric ions is not too large, and, in principle, $(\Delta V)_{||}$ may be large even without any $i_{||}$ flowing [38] (Section XII). With this model very sharp auroral arcs are expected to be associated with intensified substructures of $i_{||}$ within wider regions of weak (upward) $i_{||}$ [34,67], the intensification of $i_{||}$ being due to local reduction of the "magnetic resistance," that is, due to local transferring of electrons from the mirroring population to the precipitating population by means of gyroresonant wave-particle interaction.

According to Sharber and Heikkila [68], no systematic variation with altitude of the auroral particle energies has been observed from a few hundred km altitude to a few thousand km. This is compatible, within the accuracy of comparing observations of different events, with a widely distributed $E_{||}$, like equation (9a) (having values of at most a few mV/m close to the ionosphere; that is, as close as it actually penetrates).

Note that an $E_{||}$ according to equation (9a), for instance, allows us to apply, in a very simple manner, the model by Evans [57] in which he gives an explanation of the low-energy "continuum" spectrum of auroral electrons in terms of secondary and backscattered electrons from the ionosphere being reflected downward by a $(\Delta V)_{||}$. In Evans' model all primary electrons have energies equal to or larger than $e(\Delta V)_{||}$ [they have all fallen through the same potential $(\Delta V)_{||}$], giving rise to a pronounced high-energy peak in the energy spectrum. According to the present model (Section XI), we may expect some of the electrons with lower energies to be primary electrons that have been degraded in energy by wave-particle interactions. As the intensity and spectral shape of the backscattered and secondary electrons with lower energies are rather insensitive to the energy of the primaries (the intensity may even tend to increase with decreasing energy of the primaries [57]), we might expect essentially the same low-energy continuum if the primary high-energy peak is

"smoothed out" by wave-particle interactions. Even outside of the magnetic flux tubes with a high $(\Delta V)_{\parallel}$ there will be a residual precipitation; and if the magnetic field lines are closed, we might then find a somewhat similar low-energy continuum of electrons arriving from the conjugate ionosphere. In this manner it may be possible to reconcile the presence of a high $(\Delta V)_{\parallel}$ with the frequent observations of a fairly stable low-energy continuum even when the high-energy peak is strongly fluctuating [1, 17, 69].

As pointed out in Section X, the common collimation of electron bursts to small pitch angles [1, 21, 22] is easily understood in terms of an $E_{\parallel}$ according to equation (9a), in combination with gyroresonant waves acting as triggers of bursts (rays).

An electric field according to equation (9a) will evidently have a selective effect on a given source distribution of electrons incident at high altitudes. The electrons with lower initial energies have on the average smaller magnetic moments and will thus be more completely precipitated. As κ becomes larger in equation (9b), more high-energy electrons will be precipitated, while the precipitation of the electrons with lower energies will become successively saturated. An observer going towards the center of an inverted-V event (Fig. 3) will thus see a flattening negative slope of the electron energy spectrum above the (increasing) energy defined by $e(\Delta V)_{\parallel}$. This tendency may be further strengthened by wave-particle interactions causing the precipitating electrons to diffuse in velocity space (Section XI). Recent measurements [65] do show a similar behavior of the electron energy spectrum at low altitudes.

Arnoldy et al. [20], found field-aligned fluxes (bursts) of electrons to have distinctly lower peak energies than the accompanying isotropic and monoenergetic component. In at least one case, even the field-aligned flux appeared to be monoenergetic, although with a lower energy than the isotropic flux. It may be possible to explain these observations simply in terms of several electron populations with different energies falling through a certain $(\Delta V)_{\parallel}$, at least if all limitations of the instruments are taken into account. However, these observations fit very well into the previously mentioned model, because the gyroresonant waves that are needed to trigger bursts and rays by decreasing the magnetic moment of certain electrons will consequently lead to a reduced total energy of the collimated electrons as compared with an undisturbed isotropic component. A monoenergetic beam of collimated electrons is conceivable as a result of electrons losing most of their energy, at least their gyroenergy,

at a relatively well-defined altitude above the observer. At the same time, some electrons may lose energy by wave-particle interactions without being effectively collimated (Section XI); that is, we may not expect to find a very simple general relation among observed energies and pitch angles, particularly if velocity dispersion is likely to be important [22].

Venkatarangan et al. [70], have studied the electron pitch-angle distribution within inverted-V structures by means of a spinning satellite (the low-altitude polar orbiting satellite Isis 2). The fluxes in all energy channels were frequently found to peak at 90° pitch angles, while the lower energy flux has shown a secondary peak at small pitch angles. Since only the lower energy electrons show an increased flux at small pitch angles, we may again (in principle) ascribe to a wave-triggered collimation, which is basically associated with a certain loss of particle energy. An apparent peak flux at 90° at all energies, as seen by the spinning spacecraft (with spin period ~ 20 s) looking in only one radial direction at a time, may possibly be a temporal or spatial variation in the flux. Alternatively, the observations may be due to loss-cone distributions on closed field lines, as described in Section XII, with some electrons being scattered into the "collimation-cone" (small magnetic moments) somewhere along the field line, associated with energy loss.

Several authors [71-73] have observed very intense bursts of electromagnetic "kilometric" radiation propagating away from the Earth during the occurrence of discrete auroral forms. By direction finding technique [72,73], the radiation source has been found to be located in the auroral zones, in particular in the local evening sector, at altitudes of approximately 1 to 2 R_e above the Earth. The radiation spectrum has a peak intensity in the range 100 to 300 kHz, and the total instantaneous power of the radiation from Earth has been estimated to be as large as 1 percent of the maximum power dissipated by auroral particle precipitation [72]. In view of the estimated altitude of the source, the typical frequencies of this radiation are obviously compatible with a wave generation at the local electron gyrofrequency, in particular if we consider the effect of Doppler shifts. The present model does indeed require this kind of radiation, but we must still identify a relevant plasma-wave instability. When looking for this instability, it must be remembered that the present model may favour an instability that is operative in the absence of a dense and cold background plasma.

Rosenberg et al. [74] have observed a one-to-one correlation between bursts of VLF emissions and slightly time-delayed short bursts of x-rays (due to bursts of precipitating energetic electrons) at Siple Station, Antarctica ($L = 4.1$). From, among other things, the frequencies of the VLF emissions

(center frequency 2.5 kHz), Rosenberg et al. interpret these emissions as due to cyclotron resonance between the waves and energetic electrons at the equator, by which the wave energy is created at the expense of the electron gyroenergy. This is the same kind of wave-particle interaction assumed to occur in the present model, although the electron densities of interest in the model may be smaller than the equatorial density estimated in this case (~ 10 cm^{-3}).

Sharber and Heikkila [68] have observed, using a spinning satellite (the polar orbiting satellite Isis 1), that the electron flux in the poleward part of the nighttime auroral ovals is frequently field-aligned with a hardening of the energy spectrum at small pitch angles ("Λ" structures). When the range of the pitch angle scan is sufficiently wide, a more or less empty loss-cone may show up ("topless Λ" structures). They reject parallel electric fields as being involved and interpret their observations in terms of Fermi acceleration on closed field lines. As their observations seem to be directly related to inverted-V events, their interpretation is evidently incompatible with the above model. We are thus forced to suggest a different interpretation, although this may be somewhat ambiguous. We first notice that a hardening of the electron energy spectrum with decreasing pitch angles to a certain extent can be attributed to the loss-cone being larger for low energies than for high (cf. Fig. 7, p. 3406 of Reference 68). Such an energy-dependent loss-cone is suggested by equation (13) (Isis 1 has an apogee of 3522 km altitude). A sudden increase of $E_{\parallel}$ will, transiently (for some tens of seconds), lead to a decreased loss-cone suggested by equation (14). In particular, if the increase in $E_{\parallel}$ is relatively strong, that is, like the case $\kappa' >> \kappa$ in Section XII (κ may be zero), the velocity dispersion may well be expected to initially (within the first few seconds) cause an apparent electron energy spectrum where the peak energy is increasing towards smaller pitch angles. At the same time, the electron number flux will evidently be generally field-aligned [equations (11) and (12b)]. It is worth noting that the two paragraphs next to the last of Section XII are basically true with any $E_{\parallel}$ that is both distributed along the magnetic field line and compatible with preserved magnetic moments of the electrons. However, it may be argued that the spin period of Isis 1 (20.4 s) is somewhat too long to really permit the latter explanation of the increasing energy towards small pitch angles and the field-aligned number flux. Thus it must be assumed that the spinning spacecraft is also moving through a spatial (inverted-V) structure at the same time, or that the spacecraft is measuring a mainly temporal change in the electron energy and flux.

We further notice that even a gradually increasing $(\Delta V)_{\parallel}$, which is distributed along the magnetic field line, may cause the most energetic electrons to have the apparently smallest pitch angles at low altitude. This is because the

most energetic electrons will be the most recently accelerated at any time during the increase of $(\Delta V)_{\parallel}$. This mechanism, basically due to different starting times at a given location, is evidently an alternative to the mechanism in Section XII, which is due to different initial particle locations after a given sudden increase of $(\Delta V)_{\parallel}$. During the increase of $(\Delta V)_{\parallel}$, the velocity dispersion will evidently also cause a field-aligned number flux. The time scales involved in the low-altitude precipitation event will be determined by the growth rate of $(\Delta V)_{\parallel}$ and the actual instantaneous distribution of $E_{\parallel}$ along the magnetic field line.

Effects that may be due to a temporal or spatial variation of $(\Delta V)_{\parallel}$ are possible on open and closed magnetic field lines, but the presence of a loss-cone may seem to imply closed field lines. We note, however, that a spinning spacecraft, like Isis 1, seeing "some reduction in flux very close to $\alpha = 0°$" within an otherwise field-aligned flux may possibly be interpreted as the spacecraft seeing only the slower electrons (larger pitch angles) in a collimated and strongly velocity-dispersed electron burst. An $E_{\parallel}$, according to equation (9a), allows a collimated burst to travel very long distances with each electron keeping a constant pitch angle (Section X). If it is assumed that these bursts occur most often in the core of an inverted-V event (see Figure 3 and the comments on velocity shear instabilities in Section XV), then this kind of apparent loss-cone would be expected to show up at the peak energy, too.

The simultaneous observations of electron and (weak) proton precipitation, with even higher proton energies than electron energies, have often been used as an argument against any significant $(\Delta V)_{\parallel}$ [68,75]. For the case of the protons and electrons originating from different regions along a magnetic field-line, Block [10] has shown this to be surmountable in terms of certain distributions of $E_{\parallel}$. We do not want to restrict the above model to this case, however, but rather allow protons and electrons to originate from the same regions. The protons that are observed precipitating along with the electrons thus have been decelerated by $(\Delta V)_{\parallel}$ on their way down. The measured proton distribution does not, however, have a simple bearing on the "typical" energy distributions of protons in the source regions, as long as it is not known whether or not the charge-separation process (the dynamo) in the outer magnetosphere is associated with energy dispersion. At times a large fraction of the precipitating protons may also be previously accelerated ionospheric protons as discussed later. With an auroral proton energy typically at least as high as the electron energy [68], the proton number flux is expected to be approximately 1/40 times

the electron number flux, or larger, in the absence of a $(\Delta V)_{\parallel}$. This may be compared with, for instance, Figures 1 and 2 (p. 3400-3401) in the paper by Sharber and Heikkila [68], where the peak number flux of electrons is apparently at least three orders of magnitude larger than the simultaneous proton number flux. This evidently means that the number density of the precipitating protons is much smaller than the number density of the precipitating electrons (the proton energy seems to be somewhat reduced, too). A simple interpretation of this is that only the protons from the high-energy tail of the source distribution are able to reach lower altitudes, due to the presence of a large $(\Delta V)_{\parallel}$ in a direction to accelerate the electrons and retard the protons. The local quasi-neutrality may be maintained by upward flowing ionospheric ions. At the altitude of this particular observation (around 3000 km), upward accelerating ionospheric (topside) ions may have an energy of a few keV, depending upon the actual penetration depth of $E_{\parallel}$. However, in this particular case, the spacecraft (Isis 1) was evidently pointing in the upward direction only. The upflowing ionospheric ions will not readily be observed unless the observer is looking very close to the downward field-aligned direction.

According to Burch et al. [65], the data from Atmosphere Explorer C typically show the ratio of electron to proton energy fluxes to be strongly increased within inverted-V precipitation structures, as compared with the flux ratios outside. This would generally be expected if the electrons are being accelerated by a $(\Delta V)_{\parallel}$.

The present model leads to another interesting consequence regarding proton precipitation, or more generally, precipitation of positive ions. The parallel electric field will evidently accelerate positive ions upward from the topside ionosphere (while suppressing the ionospheric electrons). These ions will, in principle, get an extremely field-aligned velocity distribution both as a result of the diverging magnetic field lines and as a result of $E_{\parallel}$. If the magnetic field-line is closed, these energized ions may precipitate in the conjugate ionosphere together with electrons, provided $(\Delta V)_{\parallel}$ is smaller along the downward path. It is important to note that even if the electron precipitation at conjugate points is symmetric, the motion of these ions is asymmetric. While moving along the magnetic field, the ions will also drift in the transverse direction, due to centrifugal and gradient-B forces as well as due to the transverse electric field. As the travel time of a 5 keV proton, for instance, along a closed magnetic field-line at auroral latitudes will be of the order of minutes, the total $E_{\perp} \times B$ drift may evidently be several hundred km in the magnetic east-west

direction (with $E_\perp \sim 100$ mV/m at ionospheric altitudes; cf. the first paragraph of this section). Furthermore, the long travel time makes it likely that $(\Delta V)_\parallel$ will change appreciably in time (e.g., due to a changing dynamo), while the ions are traveling from one hemisphere to the other. That is, we may well expect energetic protons, as well as heavier ions [76] of ionospheric origin, to precipitate now and then together with energetic electrons. The energy of these ions may occasionally be higher than the average electron energy, in particular when $(\Delta V)_\parallel$ is rapidly decreasing in time. There may even be cases when the ions return to the original auroral display after being reflected by the $(\Delta V)_\parallel$ in the opposite hemisphere.

An interesting property of these ions is that they will generally have a field-aligned distribution also when precipitating at ionospheric altitudes. In fact, provided wave-particle interactions are unimportant, these ions will not be isotropic unless their energy is $\lesssim 1$ eV. This is because the field-alignment they got by the original upward acceleration will not be removed until they have been retarded by exactly the same potential. As a consequence, an observer at low altitudes will, on the average, find the field alignment to be more pronounced as the energy of these precipitating ions increases. In this manner the present model may be able to give a very simple alternative explanation of the fairly frequent satellite observations (ESRO/A and ESRO/B) of field-aligned fluxes of positive ions in the keV-range along with energetic (and typically isotropic) electron precipitation [77], as far as these observations can be related to closed magnetic field lines. The field alignment of these ions may, to some extent, be reduced by wave-particle interactions (see Section XI).

In the outer magnetosphere these energized ionospheric ions will evidently have a generally strong field-aligned distribution, even in the presence of a slight pitch-angle scattering, with energies of the same order as the "typical" energy of auroral electrons or lower [$(\Delta V)_\parallel \lesssim$ typical electron energies]. Furthermore, an $E_\parallel$ according to equation (9b), or more generally, any upward $E_\parallel$ that is distributed along $\bar{B}$, being basically compatible with preserved magnetic moments of the protons, will suppress the development of the loss cone of lower energy protons of magnetospheric origin, on closed magnetic field lines (see Section XII). This may explain the "source-cone" distributions of positive ions at energies less than 10 keV frequently found by the geosynchronous satellite ATS-6[1] [78].

1. DeForest, private communication.

According to DeForest,[1] and McIlwain [78], even the electrons sometimes show strong field-aligned distributions at the geosynchronous orbit (ATS-6), although much less often than the positive ions. These field-aligned electron fluxes seem to be quite intense but rather fluctuating in amplitude (on a time scale of a quarter of a second, according to DeForest). The energy spectrum of these electrons is typically rather flat or slightly rising up to a break point somewhere between 0.1 and 10 keV, beyond which it rapidly decreases. Field-aligned distributions with break-point energies greater than 2 keV seem to occur only within the first 10 min after the onset of a "substorm injection" [78]. It might be tempting to associate these electron "beams" with a downward current (upward moving electrons) like B-C in Figure 4. As we normally expect a downward current to be easily carried by upward escaping cold ionospheric electrons [14,15], we then have to invoke some kind of current obstruction, e.g., a double layer [10,40]. However, there may be other explanations more closely related to the present model. For instance, if the cold plasma has been previously depleted at high altitudes by an upward current, a downward current of upflowing ionospheric electrons will be space-charge limited and associated with a downward $E_{||}$ [52]. Another conceivable explanation is the following.

Consider equations (9b) through (11). Suppose the electric field (9b) is turned off. All electrons along the magnetic field line then suddenly experience an increased upward force, and we have a situation analogous to one with a hot gas inside a rocket nozzle. Here the hottest gas is initially in the innermost portion of the "magnetic nozzle." The electrons with the smallest pitch angles will still be able to precipitate, but the major portion of the electrons in the region of strong magnetic field (within one or two earth radii above the ionosphere) will evidently "blow out" (upwards) of the "nozzle," while transforming their gyromotion into directional (field-aligned) motion.

In this way, a short-duration burst (a few seconds or less for keV energies) of field-aligned electrons may appear at a geosynchronous orbit, having energies up to a certain limit, determined by the original $(\Delta V)_{||}$ (we may have to assume that the loss cone gets filled by scattering). However, we may, in principle, even have a more persistent outflow of such field-aligned electrons. This is because a current loop (e.g., ABCD in Figure 4) is basically a "resonant circuit," the "inductance" being due to the encircled magnetic field and the "capacitance" being due to the charged-particle convection through the loop [79]. That is, transient currents can flow across the magnetic field anywhere between A and D in the form of polarization currents. For the present application, point A is considered to be located in the midnight sector. Suppose that the supply of electrons (and protons) at point A in Figure 4 is drastically increased following a "substorm injection." This may tend to short-circuit the

$(\Delta V)_{\parallel}$ along A-D due to the increased number of electrons with small magnetic moments (provided the dynamo voltage V(A-B) does not increase too much at the same time), enabling energized electrons from lower altitudes to escape upwards (after being mirrored) without being appreciably retarded, thus forming a field-aligned beam. This may tend to reduce, or even reverse, $i_{\parallel}$ at lower altitudes, which may cause the magnetic induction to increase $E_{\parallel}$ again. New electrons arriving from high altitudes become strongly collimated by the increased $E_{\parallel}$ leading to a high $i_{\parallel}$, etc. At least from these highly speculative arguments, one might expect (fluctuating) beams of field-aligned and energized electrons to occur at geosynchronous altitudes for periods appreciably longer than a few seconds. The conjugate current loop still has to be considered. However, a further study of this very complicated problem is far beyond the scope of this paper. The fact that electron and positive-ion beams at high energy do not seen to occur simultaneously [78] may be interpreted as due to the upward moving ionospheric ions not being appreciably accelerated under these circumstances because of their large mass.

Note that this kind of oscillating energization of the electrons has to be associated with pulsating auroras [80,81]. These phenomena seem to occur (from late evening to dawn) somewhat equatorward of a magnetic dipole field-line through ATS-6 (at 94°W longitude). However, the disturbed (tail-like) shape of the geomagnetic field may compensate for this in the midnight sector. Actually, the observations of field-aligned electron beams, reported so far [78], occurred in this local time sector. Besides, the observations of large intensity fluctuations (at given energy) in the frequency range from one to a few hertz (cf. Fig. 10, p. 16, in Reference 78) are evidently compatible with typical "frequencies" of auroral brightness fluctuations [80].

When the positive ionospheric (topside) ions are accelerated upward by a steady $E_{\parallel}$ [e.g. equation (9b)], they also are reduced in density as compared with the density distribution of freely escaping ions. Consequently, the high-altitude density of ionospheric electrons has to be correspondingly reduced to preserve charge neutrality which is automatically accomplished by $(\Delta V)_{\parallel}$ depressing the topside electrons and replacing these with a dilute population of precipitating, backscattered, and (energetic) secondary electrons. This reduction of the electron (and ion) density in the uppermost ionosphere and lower magnetosphere may be compatible with the frequent Alouette II observations [82] of very low electron concentrations at high latitudes ($L \gtrsim 6$) and high altitudes (1500 to 3000 km).

At lower altitudes within the ionosphere, an electric field like equation (9a) is expected, having a maximum strength of a few times 1 mV/m, to be largely screened out by the collision-dominated ionospheric plasma. The actual depth of penetration will evidently determine the ion-composition in the upward flux of positive ions. In a case where O^+ and N^+ ions are being effectively accelerated, we may expect these to have a larger density than the protons even at high altitudes because of their smaller velocities. This may seem to be compatible with mass spectrometer data presented by Hoffman [83] which show O^+ and N^+ to be the dominant ions at 3000 km above the auroral zone at certain times.

Direct observations of $E_{\parallel}$ have actually been reported [84, 85]. These observations have been made at altitudes of only a few hundred km within and above auroral arcs. The electric field component along the magnetic field has been directed downward in all cases and has been as large as 20 mV/m. These observations are somewhat puzzling, but the following qualitative explanation is suggested. The horizontal current C-D in Figure 4 is a Pedersen current (carried mostly by positive ions [43]) distributed over a certain altitude range in the lower ionosphere. A non-negligible fraction of this current flows at altitudes several hundred km above the altitudes where the energetic precipitating electrons are (finally) deposited at D [43]. Because these electrons carry the upward part D-A of the current loop, this might be expected to result in a downward (decelerating) $E_{\parallel}$ in the wake of the precipitating electrons. To explain the large magnitude of the observed $E_{\parallel}$, "anomalous resistivity" is invoked. As found theoretically by Papadopoulos and Coffey [86], the precipitating electrons may excite parametric instabilities in the ionospheric plasma that may appreciably enhance the resistivity.

XV. SUMMARY AND CONCLUDING REMARKS

The existence of field-aligned currents associated with auroral precipitation (Section IV) suggests a process of charge separation (a dynamo) in the distributions of "hot" particles in the outer magnetosphere and the magnetosphere-solar wind transition region (Section XIII), leading to current loops like ABCD in Figure 4, for instance. The downward current B-C may generally be carried by escaping ionospheric electrons, charging point C positive to essentially the same potential as point B. A Pedersen current C-D will charge point D positive relative to point A. However, the upward current D-A will generally have to be

carried by down-flowing hot magnetospheric electrons which do not readily flow because of the magnetic mirroring (Section VIII). This may lead to a large $(\Delta V)_{\parallel}$ along A-D, entirely due to adiabatic particle motion, that will increase the number flux of precipitating electrons as well as the kinetic energy (Sections VIII through X). At the same time, this $(\Delta V)_{\parallel}$ will energize outflowing positive ionospheric ions (Section XIV). A region of high $(\Delta V)_{\parallel}$ generally has to be rather wide in latitude as well as longitude (Section V), which requires an additional mechanism for producing auroral fine structures. For this reason, wave-particle interactions are invoked as a mechanism by which electrons can lose energy (primarily to the waves). Any spatially localized wave-particle interaction that appreciably reduces at least the gyroenergy of downflowing electrons will automatically lead to a locally intensified and often strongly collimated precipitation, like auroral rays (Sections IX through X).

In this model the parallel electric field (in reality the dynamo) provides the increased energy flux in auroral displays, whereas the spatial structure of individual auroral forms may be due to a modulating effect of certain kinds of plasma instabilities. These plasma instabilities may not provide "anomalous resistivity," however. On the contrary, these instabilities may tend to limit the growth of $(\Delta V)_{\parallel}$ by their thermalizing effect on the otherwise adiabatic particle motion.

The association of a net field-aligned current with precipitating electrons also suggests that the convection electric field $E_{\perp}$ is (generally) transverse to auroral arcs (cf. observations made in References 45 and 47) with steep gradients within the precipitation structure (Sections VI and VII), particularly at altitudes from a few to several thousand km [Fig. 3 and equation (9a)]. The resulting $E_{\perp} \times B$ drift pattern is seemingly likely to lead to different kinds of shear flow instabilities, similar to the Kelvin-Helmholtz instability, that may generate folds and vortex-forms [67, 87]. The frequent alignment of thin auroral forms along the $E_{\perp} \times B$ drift direction [67] might indicate that the gyroresonant waves assumed in this model (that is, waves resonating with the (Doppler-shifted) electron gyrofrequency) are closely related to the $E_{\perp}$-field and, perhaps, such shear flow instabilities.

REFERENCES

1. O'Brien, B. J., and D. L. Reasoner, Measurements of Highly Collimated Short-Duration Bursts of Auroral Electrons and Comparison with Existing Auroral Models, J. Geophys. Res., 76, 8258, 1971.

2. Kennel, C. F., and H. E. Petschek, Limit on Stably Trapped Particle Fluxes, J. Geophys. Res., 71, 1, 1966.

3. Vasyliunas, V. M., Low Energy Particle Fluxes in the Geomagnetic Tail, in The Polar Ionosphere and Magnetospheric Processes, ed. G. Sklovi, Gordon and Breach, New York, 1970.

4. Frank, L. A., Relationship of the Plasma Sheet, Ring Current, Trapping Boundary, and Plasmasphere near the Magnetic Equator and Local Midnight, J. Geophys. Res., 76, 2265, 1971.

5. Heikkila, W. J., Outline of a Magnetospheric Theory, J. Geophys. Res., 79, 2496, 1974.

6. Perkins, F. W., Plasma-Wave Instabilities in the Ionosphere Over the Aurora, J. Geophys. Res., 73, 6631, 1968.

7. Gary, S. P., D. Montgomery, and D. W. Swift, Particle Acceleration by Electrostatic Waves with Spatially Varying Phase Velocities, J. Geophys. Res., 73, 7524, 1968.

8. Laval, G., and R. Pellat, Particle Acceleration by Electrostatic Waves Propagating in an Inhomogeneous Plasma, J. Geophys. Res., 75, 3255, 1970.

9. Swift, D. W., Particle Acceleration by Electrostatic Waves, J. Geophys. Res., 75, 6324, 1970.

10. Block, L. P., Potential double layers in the ionosphere, Cosmic Electrodynamics, 3, 349, 1972.

11. Swift, D. W., On the Formation of Auroral Arcs and Acceleration of Auroral Electrons, J. Geophys. Res., 80, 2096, 1975.

12. Swift, D. W., A Mechanism for Energizing Electrons in the Magnetosphere, J. Geophys. Res., 70, 3061, 1965.

REFERENCES (Continued)

13. Kindel, J. M., and C. F. Kennel, Topside Current Instabilities, J. Geophys. Res., 76, 3055, 1971.

14. Knight, S., Parallel electric fields, Planet. Space Sci., 21, 741, 1973.

15. Lemaire, J., and M. Scherer, Plasma sheet particle precipitation: a kinetic model, Planet. Space Sci., 21, 281, 1973.

16. Lemaire, J., and M. Scherer, Ionosphere-plasmasheet field-aligned currents and parallel electric fields, Planet. Space Sci., 22, 1485, 1974.

17. Westerlund, L. H., The Auroral Electron Energy Spectrum Extended to 45 eV, J. Geophys. Res., 74, 351, 1969.

18. Albert. R. D., and P. J. Lindstrom, Auroral-Particle Precipitation and Trapping Caused by Electrostatic Double Layers in the Ionosphere, Science, 170, 1398, 1970.

19. Choy, L. W., R. L. Arnoldy, W. Potter, P. Kintner, and L. J. Cahill, Jr., Field-Aligned Particle Currents near an Auroral Arc, J. Geophys. Res., 76, 8279, 1971.

20. Arnoldy, R. L., P. B. Lewis, and P. O. Isaacson, Field-Aligned Auroral Electron Fluxes, J. Geophys. Res., 79, 4208, 1974.

21. Hoffman, R. A. and D. S. Evans, Field-Aligned Electron Bursts at High Latitudes Observed by Ogo-4, J. Geophys. Res., 73, 6201, 1968.

22. Whalen, B. A., and I. B. McDiarmid, Observations of Magnetic Field-Aligned Auroral-Electron Precipitation, J. Geophys. Res., 77, 191, 1972.

23. Ackerson, K. L., and L. A. Frank, Correlated Satellite Measurements of Low-Energy Electron Precipitation and Ground-Based Observations of a Visible Auroral Arc, J. Geophys. Res., 77, 1128, 1972.

24. Bosqued, J. M., G. Cardona, and H. Réme, Auroral Electron Fluxes Parallel to the Geomagnetic Field Lines, J. Geophys. Res., 79, 98, 1974.

REFERENCES (Continued)

25. Frank, L. A., and K. L. Ackerson, Observations of Charged Particle Precipitation into the Auroral Zone, J. Geophys. Res., 76, 3612, 1971.

26. Cauffman, D. P., and D. A. Gurnett, Satellite Measurements of High Latitude Convection Electric Fields, Space Science Rev., 13, 369, 1972.

27. Wescott, E. M., J. R. Kan, H. C. Stenbaek-Nielsen, and H. M. Peek, Fast Barium Plasma Flux Tube Interaction with Auroral Electron Flux Beyond 1 R_e, Transactions, American Geoph. Union, 56, 1170, 1974.

28. Zmuda, A. J., J. C. Armstrong, and F. T. Heuring, Characteristics of Transverse Magnetic Disturbances Observed at 1100 km in the Auroral Oval, J. Geophys. Res., 75, 4757, 1970.

29. Armstrong, J. C., and A. J. Zmuda, Field-Aligned Current at 1100 km in the Auroral Region Measured by Satellite, J. Geophys. Res., 75, 7122, 1970.

30. Zmuda, A. J., and J. C. Armstrong, The Diurnal Variation of the Region with Vector Magnetic Field Changes Associated with Field-Aligned Currents, J. Geophys. Res., 79, 2501, 1974.

31. Park, R. J., and P. A. Cloutier, Rocket-Based Measurement of Birkeland Currents Related to an Auroral Arc and Electrojet, J. Geophys. Res., 76, 7714, 1971.

32. Cloutier, P. A., B. R. Sandel, H. R. Anderson, P. M. Pazich, and R. J. Spiger, Measurements of Auroral Birkeland Currents and Energetic Particle Fluxes, J. Geophys. Res., 78, 640, 1973.

33. Berko, F. W., R. A. Hoffman, R. K. Burton, and R. E. Holzer, Simultaneous Particle and Field Observations of Field-Aligned Currents, J. Geophys. Res., 80, 37, 1975.

34. Armstrong, J. C., S. I. Akasofu, and G. Rostoker, A Comparison of Satellite Observations of Birkeland Currents with Ground Observations of Visible Aurora and Ionospheric Currents, J. Geophys. Res., 80, 575, 1975.

REFERENCES (Continued)

35. Kan, J. R., Energization of Auroral Electrons by Electrostatic Shock Waves, J. Geophys. Res., 80, 2089, 1975.

36. Buneman, O., Dissipation of Currents in Ionized Media, Phys. Rev. 115, 503, 1959.

37. Alfvén, H., and C. G. Fälthammar, Cosmic Electrodynamics, Fundamental Principles, 2nd Edn., Oxford University Press, London, 1963.

38. Persson, H., Electric Field along a Magnetic Line of Force in a Low-Density Plasma, Phys. Fluids, 6, 1756, 1963.

39. Persson, H., Electric Field Parallel to the Magnetic Field in a Low-Density Plasma, Phys. Fluids, 9, 1090, 1966.

40. Block, L. P., Double Layers, paper presented at the Nobel Symposium on the Physics of the Hot Plasmas in the Magnetosphere at the Geophys. Inst. in Kiruna, Sweden, April 2-4, 1975, techn. rep. TRITA-EPP-75-10, Department of Plasma Physics, Royal Inst. of Technology, S-10044 Stockholm, 1975.

41. Cummings, W. D., R. J. O'Sullivan, and P. J. Coleman, Jr., Standing Alfvén Waves in the Magnetosphere, J. Geophys. Res., 74 , 778, 1969.

42. Chamberlain, J. W., Physics of the Aurora and Airglow, Academic Press, New York and London, p. 124, 1961.

43. Boström, R., A Model of the Auroral Electrojets, J. Geophys. Res., 69, 4983, 1964.

44. Aggson, T. L., Probe Measurements of Electric Fields in Space, in Atmospheric Emissions, ed. by B. M. McCormac and A. Omholt, p. 305, Van Norstrand Reinhold Co., New York, 1969.

45. Wescott, E. M., J. D. Stolarik, and J. P. Heppner, Electric Fields in the Vicinity of Auroral Forms from Motions of Barium Vapor Releases, J. Geophys. Res., 74, 3469, 1969.

46. Potter, W. E., Rocket Measurements of Auroral Electric and Magnetic Fields, J. Geophys. Res., 75, 5415, 1970.

REFERENCES (Continued)

47. Gurnett, D. A., and L. A. Frank, Observed Relationship between Electric Fields and Auroral Particle Precipitation, J. Geophys. Res., 78, 145, 1973.

48. Lennartsson, W., On high-latitude convection field inhomogeneities, Birkeland currents and inverted "V" precipitation events, techn. rep. TRITA-EPP-73-11, Department of Plasma Physics, Royal Inst. of Technology, S-10044, Stockholm, 1973.

49. Biskamp, D., and R. Chodura, Asymptotic behavior of the two-stream instability, Phys. Fluids, 16, 888, 1973.

50. Lemaire, J., and M. Scherer, Kinetic Models of the Solar and Polar Winds, Rev. of Geophys. and Space Phys., 11, 427, 1973.

51. Chappell, C. R., Recent Satellite Measurements of the Morphology and Dynamics of the Plasmasphere, Rev. of Geophys. and Space Phys., 10, 951, 1972.

52. Block, L. P., Coupling Between the Outer Magnetosphere and the High-Latitude Ionosphere, Space Science Rev., 7, 198, 1967.

53. Stix, T. H., The Theory of Plasma Waves, McGraw-Hill, New York, 1962.

54. Helliwell, R. A., A Theory of Discrete VLF Emissions from the Magnetosphere, J. Geophys. Res., 72, 4773, 1967.

55. Hess, W. N., M. C. Trichel, T. N. Davis, W. C. Beggs, G. E. Kraft, E. Stassinopoulos, and E. J. R. Maier, Artificial Aurora Experiment: Experiment and Principal Results, J. Geophys. Res., 76, 6067, 1971.

56. Jones, T. W., and P. J. Kellogg, Plasma Waves Artificially Induced in the Ionosphere, J. Geophys. Res., 78, 2166, 1973.

57. Evans, D. S., Precipitating Electron Fluxes Formed by a Magnetic Field-Aligned Potential Difference, J. Geophys. Res., 79, 2853, 1974.

58. Aubry, M. P., M. G. Kivelson, R. L. McPherron, C. T. Russell, and D. S. Colburn, Outer Magnetosphere near Midnight at Quiet and Disturbed Times, J. Geophys. Res., 77, 5487, 1972.

REFERENCES (Continued)

59. Alfvén, H., Electric current structure of the magnetosphere, Introductory lecture at the Nobel Symposium on the Physics of the Hot Plasma in the Magnetosphere at the Geophysical Institute in Kiruna, Sweden, April 2-4, 1975, techn. rep. TRITA-EPP-75-03, Dep. of Plasma Physics, Royal Inst. of Techn., S-10044 Stockholm 70, Sweden, 1975.

60. Jaggi, R. K., and R. A. Wolf, Self-Consistent Calculation of the Motion of a Sheet of Ions in the Magnetosphere, J. Geophys. Res., 78, 2852, 1973.

61. Frank, L. A., and D. A. Gurnett, Distributions of Plasmas and Electric Fields over the Auroral Zones and Polar Caps, J. Geophys. Res., 76, 6829, 1971.

62. Heppner, J. P., Electric Field variations during substorms: Ogo-6 measurements, Planet. Space Sci., 20, 1475, 1972.

63. Heppner, J. P., High latitude electric fields and the modulations related to interplanetary magnetic field parameters, Radio Sci., 8, 933, 1973.

64. Gurnett, D. A., and S. I. Akasofu, Electric and Magnetic Field Observations During a Substorm on February 24, 1970, J. Geophys. Res., 79, 3197, 1974.

65. Burch, J. L., S. A. Fields, W. B. Hanson, R. A. Heelis, and R. A. Hoffman, Characteristics of Auroral Electron Acceleration Regions Observed by Atmosphere Explorer C, submitted to J. Geophys. Res., 1975.

66. Hanson, W. B., D. R. Zuccaro, C. R. Lippincott, and S. Sanatani, The retarding-potential analyzer on Atmopheric Explorer, Radio Sci., 8, 333, 1973.

67. Hallinan, T. J., and T. N. Davis, Small-scale auroral arc distortions, Planet. Space Sci., 18, 1735, 1970.

68. Sharber, J. R., and W. J. Heikkila, Fermi Acceleration of Auroral Particles, J. Geophys. Res., 77, 3397, 1972.

69. Reasoner, D. L., and C. R. Chappell, Twin Payload Observations of Incident and Backscattered Auroral Electrons, J. Geophys. Res., 78, 2176, 1973.

REFERENCES (Continued)

70. Venkatarangan, P., J. R. Burrows, and I. B. McDiarmid, On the Angular Distributions of Electrons in "Inverted-V" Substructures, J. Geophys. Res., 80, 66, 1975.

71. Dunckel, N., B. Ficklin, L. Rorden, and R. A. Helliwell, Low-Frequency Noise Observed in the Distant Magnetosphere with Ogo-1, J. Geophys. Res., 75, 1854, 1970.

72. Gurnett, D. A., The Earth as a Radio Source: Terrestrial Kilometric Radiation, J. Geophys. Res., 79, 4227, 1974.

73. Kurth, W. S., M. M. Baumback, and D. A. Gurnett, Direction-Finding Measurements of Auroral Kilometer Radiation, J. Geophys. Res., 80, 2764, 1975.

74. Rosenberg, T. J., R. A. Helliwell, and J. P. Katsufrakis, Electron Precipitation Associated with Discrete Very-Low-Frequency Emissions, J. Geophys. Res., 76, 8445, 1971.

75. O'Brien, B. J., Considerations that the source of auroral energetic particles is not a parallel electrostatic field, Planet. Space Sci., 18, 1821, 1970.

76. Shelley, E. G., R. G. Johnson, and R. D. Sharp, Satellite Observations of Energetic Heavy Ions During a Geomagnetic Storm, J. Geophys. Res., 77, 6104, 1972.

77. Hultquist, B., On the production of a magnetic-field-aligned electric field by the interaction between the hot magnetospheric plasma and the cold ionosphere, Planet. Space Sci., 19, 749, 1971.

78. McIlwain, C. E., Auroral electron beams near the magnetic equator, presented at the Nobel Symposium on the Physics of the Hot Plasma in the Magnetosphere at the Geophys. Inst. in Kiruna, Sweden, April 2-4, 1975, to be published Proceedings Plenum Press, London.

79. Lennartsson, W., Ionospheric electric field and current distribution associated with high altitude electric field inhomogeneities, Planet. Space Sci., 21, 2089, 1973.

REFERENCES (Concluded)

80. Shepherd, G. G., and E. V. Pemberton, Characteristics of Auroral Brightness Fluctuations, Radio Sci., 3, 650, 1968.

81. Cresswell, G. R., The morphology of displays of pulsating auroras, J. Atmosph. and Terrestrial Phys., 34, 549, 1972.

82. Hagg, E. L., Electron Densities of 8-100 Electrons cm^{-3} Deduced from Alouette II High-Latitude Ionograms, Canadian J. of Phys. 45, 27, 1966.

83. Hoffman, J. H., Ion Composition Measurements in the Polar Region from the Explorer 31 Satellite, Trans. Am. Geophys. Union, 49, 253, 1968.

84. Mozer, F. S., and U. V. Fahleson, Parallel and perpendicular electric fields in aurora, Planet. Space Sci., 18, 1563, 1970.

85. Kelley, M. C., F. S. Mozer, and U. V. Fahleson, Electric Fields in the Nighttime and Daytime Auroral Zone, J. Geophys. Res., 76, 6054, 1971.

86. Papadopoulos, K., and T. Coffey, Anomalous Resistivity in the Auroral Plasma, J. Geophys. Res., 79, 1558, 1974.

87. Haerendel, G., A Note on Shear Flows in the Magnetosphere, Trans. Am. Geoph. Union, 55, 1005, 1974.

APPROVAL

SKETCH OF A UNIFYING AURORAL THEORY

The information in this report has been reviewed for security classification. Review of any information concerning Department of Defense or Atomic Energy Commission programs has been made by the MSFC Security Classification Officer. This report, in its entirety, has been determined to be unclassified.

This document has also been reviewed and approved for technical accuracy.

Charles Richard Chappell

CHARLES R. CHAPPELL
Chief, Magnetospheric and Plasma Physics Branch

Rudolf Decher

RUDOLF DECHER
Chief, Radiation and Low Temperature Sciences Division

Charles A. Lundquist

CHARLES A. LUNDQUIST
Director, Space Sciences Laboratory

☆U.S. GOVERNMENT PRINTING OFFICE 1976-641-255/402 REGION NO. 4